Occurrence and Characterization of Mn Nodules in a Toposequence at Coloso Valley Agricultural Reserve

by

Sherlynette Pérez Castro

A thesis submitted in partial fulfillment of the requirements for the degree of

MASTER OF SCIENCE
in
SOIL SCIENCES

UNIVERSITY OF PUERTO RICO
MAYAGÜEZ CAMPUS
2010

Approved by:

_____	_____
Winston de la Torre, PhD Member, Graduate Committee	Date
_____	_____
Julia M. O'Hallorans, PhD Member, Graduate Committee	Date
_____	_____
Miguel A. Muñoz, PhD President, Graduate Committee	Date
_____	_____
Ricardo R. López, PhD Representative of Graduate Studies	Date
_____	_____
Hipólito O'Farrill, PhD Chairperson of the Department	Date

Abstract

Manganese (Mn) nodules are sedimentary rocks, generally spherical or irregularly round in shape with concentric layers formed from manganese and iron mineral precipitation. These are redoximorphic features in soils with fluctuating high water table. This study aimed to: (i) evaluate taxonomically the soil profiles, (ii) determine the occurrence of manganese nodules in the soil horizons, (iii) evaluate physical and chemical properties of Mn nodules, and (iv) theorize about manganese nodules formation mechanism in the Coloso Valley Agricultural Reserve. A toposequence comprising three soil series, Rio Piedras (Typic Hapludults), Bajura (Vertic Endoaquolls), and Coloso (Vertic Dystrudepts) was selected for the study. The largest Mn nodules were observed in the Ap horizon of the Rio Piedras soil series; however this site had the fewest nodules. Two grams of manganese nodules per 800 g of soil were observed. In Bajura and Coloso soil series, the largest occurrence of manganese nodules was observed in the Bwg horizon. The nodule mass in Bajura soil was 11 g/800 g and in Coloso soil it was 15 g/800 g. Manganese nodules from Rio Piedras soil were well formed with clearly defined concentric layers. In Coloso and Bajura soils the Mn nodules were not well formed and irregular masses of Mn oxides were observed on soil peds. XRD analyses of manganese nodules from the three soils indicate the presence of lithiophorite and todorokite. Coloso and Bajura soils occur at the lower levels in the toposequence, where they are subjected to wet and dry cycles. In Bajura and Coloso soils a more active redox process of Mn is taking place. This process results in the formation of small manganese nodules and masses. Rio Piedras soil occurs at higher elevation and the water table never saturates the soil profile. The highest rate of oxidation creates stability and well formed nodules. The presence of Mn nodules in the Ap horizon of Rio Piedras soil indicates

significant changes in hydrologic conditions in this toposequence, suggesting a soil uplifting event.

Resumen

Los nódulos de manganeso (Mn) son rocas sedimentarias generalmente esféricas o irregularmente redondas caracterizadas por la presencia de láminas concéntricas formadas por óxidos de Mn, en láminas alternadas con óxidos de hierro. Éstos son estructuras redoximórficas en suelos con un nivel freático fluctuante. Este estudio tuvo como objetivo: (i) evaluar taxonómicamente los perfiles de suelo (ii) determinar la incidencia de nódulos de Mn en los horizontes de los suelos, (iii) evaluar las propiedades físicas y químicas de los nódulos de Mn y (iv) teorizar sobre los mecanismos de formación de los nódulos de Mn en la Reserva Agrícola del Valle Coloso. Una toposecuencia compuesta por tres series de suelo, Río Piedras (Typic Hapludults), Bajura (Vertic Endoaquolls) y Coloso (Vertic Dystrudepts), fue seleccionada para el estudio. Se observó que los nódulos de Mn de mayor tamaño se encontraban en el horizonte Ap de la serie de suelo Río Piedras, sin embargo su incidencia fue menor. Dos gramos de nódulos de manganeso por 800 g de suelo fueron observados. En las series de suelo Bajura y Coloso, se observó la mayor incidencia de nódulos de manganeso en el horizonte Bwg. La masa de nódulos en el suelo Bajura fue de 11 g/800 g y en Coloso fue de 15 g/800 g de suelo. Los nódulos de manganeso del suelo Río Piedras estaban bien formados y con capas concéntricas claramente definidas. En los suelos Coloso y Bajura los nódulos de Mn no estaban bien formados y se observaron masas irregulares en los agregados del suelo. El análisis de difracción de rayos X de los nódulos de manganeso indicó la presencia de litioforita y todoroquita en los tres suelos. Los suelos Coloso y Bajura se encuentran en los niveles más bajos de la toposecuencia, donde están expuestos a fluctuaciones del nivel freático con mayor frecuencia. En los suelos Bajura y Coloso reacciones de reducción y oxidación de Mn son más activas. Este proceso resulta en la formación de pequeños nódulos y masas de manganeso. El suelo Río Piedras se encuentra a mayor

elevación y el nivel freático no satura el perfil del suelo. La mayor tasa de oxidación crea estabilidad y nódulos bien formados. La presencia de nódulos de manganeso en el horizonte Ap del suelo Río Piedras indica cambios significativos en las condiciones hidrológicas en esta toposecuencia, y sugiere un posible levantamiento del terreno.

To Janette Castro Quintero

Acknowledgements

During the development of my graduate studies several people and institutions collaborated with my research. Without their support has been impossible to complete my work. That is why I want to dedicate this section to recognize their support.

I want to express sincere acknowledgement to my advisor Dr. Miguel A. Muñoz for giving me the opportunity to conduct research under his guidance and supervision. I greatly appreciate his encouragement and support during all my studies. I also want to thank the support received from USDA-NRCS Mayagüez MLRA Soil Survey Office soil scientists Jorge Lugo and Samuel Ríos. Special thanks to Dr. Stefanie Whitmire and Dr. Julia M. O'Hallorans for their reviews and helpful comments. I also thank Mr. Freddy Patiño, Mr. Ulises Chardón, Dr. Lysa Chizmadia, and Dr. Alejandro Segarra Carmona for their collaborations.

The Grant from USDA-Hispanic Serving Institutions Program, project # 2008-38422-19138 provided the funding and the resources for the development of this research. I would like to thank my family and friends for their inspiration and love.

Table of Contents

List of tables

List of figures

1 Introduction

Manganese (Mn) nodules are sedimentary rocks, generally spherical or irregularly round in shape with concentric layers formed from manganese and iron mineral precipitation. They are the major depositional form of Mn and Fe in oceans, lakes and soils (Wen-Fen, et. al., 2006; Burns, 1976; Burns and Burns, 1975; Dixon and Skinner, 1992; McKenzie, 1989). Concretion formation is influenced by soil environments alternating between flooded anaerobic conditions and dryer aerobic conditions. During wet periods, Mn is reduced and dissolves in pore waters, while during dry periods it reprecipitates and cements soil particles (Tebo et. al., 1998). Repetition of this process eventually forms millimeter – size nodules that often exhibit the concentric layering suggestive of seasonal growth (Manceau et. al., 2003).

The presence of manganese nodules in agricultural fields affects: (1) the availability of labile manganese, (2) the presence of the different valence states of manganese and their roles as electron donors or acceptors in oxidation and reduction reactions (Gambrell, 1996), and (3) the availability of both nutritious and toxic trace metals to plants, due to manganese oxides/hydroxides high absorbent capacity for heavy-metals (Negra et. al., 2005a).

In Puerto Rico manganese nodules have never been studied in terms of its quantification and/or characterization. This research presents the basis to understand the occurrence of manganese nodules in the soils of the Coloso Valley. We presented them not only as a valuable source of information about the mineralogy and geochemistry of Mn oxides in soils, but also as indicators

of soil drainage, pH, parent material, maturity and nutritious and toxic trace metals availability and their environmental impact for vegetative, soil and aquatic environments.

2 Literature Review

Manganese (Mn) is the 12th most abundant element in the Earth's crust and is an essential trace metallic element for plant nutrition. The main defined function of manganese in plants is during the first stage of photosynthesis (light reactions) when water is oxidized to oxygen by Mn ions (Mn^{+2}) (Taiz and Zeiger, 2002). Manganese also activates several enzymes such as decarboxylases and dehydrogenases involved in the citric acid cycle. Manganese gets to the soil solution from the depletion of rocks, by their interactions with surface water, forming soluble, exchangeable, adsorbed or by reprecipitation insoluble manganese. Soil pH and reduction potential are the primary factors affecting Mn chemical form. Waterlogged conditions and/or pH levels below six favor reduction to the more mobile and plant available divalent Mn (Mn^{+2}), while higher pH and oxidized soil conditions favor Mn^{+2} oxidation to the Mn^{+4} form which is generally found in insoluble oxides in soils (Figure 2.1). A variety of Mn oxide minerals occur in different soils. Birnessite, todorokite, lithiophorite, and hollandite are being reported as the most common (Table

Figure 2.1 Fields of stability of Mn species in aqueous solution (Hem, 1963)

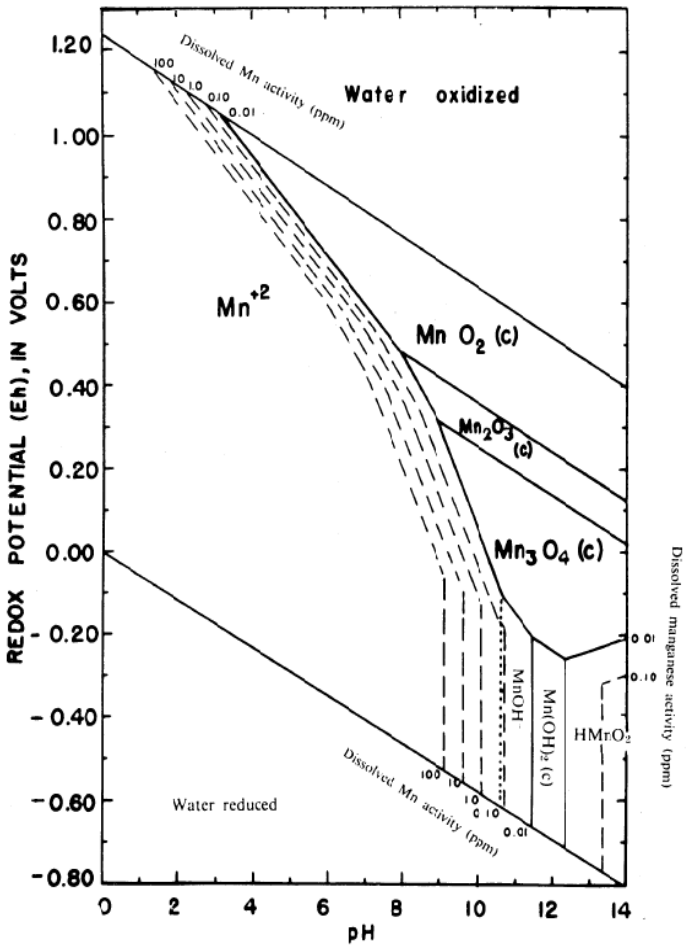

2.1). During pedogenesis manganese oxides can accumulate forming redoximorphic features such as masses, concretions and nodules. Masses are noncemented bodies of various shapes that cannot be removed as discrete units. Concretions and nodules are cemented bodies that can be removed as discrete units from soil. Nodules present concentric layers of material around a point, line, or plane and.

The presence of manganese masses, concretions and nodules has been investigated with different approaches. One approach studies its occurrence and physical properties for taxonomic evaluations. The USDA-NRCS *Field Book for Describing and Sampling Soils* records them as concentrations or redoximorphic features. Physical properties such as type, quantity, size and color are evaluated. Iron and Mn commonly occur in combination, but Mn features slightly effervess with hydrogen peroxide (H_2O_2). This effervescence comes from the products of hydrogen peroxide decomposition catalyzed by manganese oxide ($2H_2O_2 \xrightarrow{MnO_2} O_2 + 2H_2O$). Another approach evaluates the soil environment necessary for the

Table 2.1 Manganese oxide minerals (Dixon & White, 2002)

Mineral or synthetic equivalent	Chemical formula
Birnessite	$(Na, Ca, Mn^{2+})Mn_7O_{14} \bullet 2.8H_2O$
Buserite	$Na_4Mn_{14}O_{27} \bullet 21H_2O$
Chalcophanite	$ZnMn_3O_7 \bullet 21H_2O$
Coronadite	$Pb_x(Mn^{4+}Mn^{3+})_8O_{16}(x = 1-1.4)$
Cryptomelane	$K_x(Mn^{4+}Mn^{3+})_8O_{16}(x = 1.3-1.5)$
Hausmannite	Mn_3O_4
Hollandite	$Ba_x(Mn^{4+}Mn^{3+})_8O_{16}(x = 1)$
Lithiophorite	$(Al, Li)MnO_2(OH)_2$
Manganite	$MnOOH$
Nsutite	$Mn^{4+}Mn^{3+}(O, OH)_2$
Pyrolusite	MnO_2
Ramsdellite	MnO_2
Rancieite	$(Ca, Mn)Mn_4O_9 \bullet nH_2O$
Romanechite	$Ba_{0.66}(Mn^{4+}Mn^{3+})_5O_{10} \bullet 1.34H_2O$
Todorokite	$(Na, Ca, K)_{0.3-0.5}(Mn^{4+}Mn^{3+})_5O_{12} \bullet 3.5H_2O$
Vernadite	$MnO_2 \bullet nH_2O$

accumulation of manganese oxides. Alternating flooded anaerobic conditions and dryer aerobic conditions has been reported as the main process for concretion formation. During wet periods, Mn is reduced and dissolved in pore water, while during dry periods they re-precipitate and accumulate through microbial oxidation and auto-oxidation of Mn^{+2} (Wen-Feng et. al., 2006; Sullivan and Koppi, 1992). Repetition of this process eventually forms millimeter – size nodules that often exhibit the concentric layering suggestive of seasonal growth (Manceau et. al., 2003). Since these conditions occur at different intensities in each type of soil and even along the soil profile, the manganese features in each soil will vary in occurrence, and physical and chemical properties. Soil properties such as parent material, texture, pH, manganese concentrations, maturity, and landscape position influence manganese oxides of accumulation. For example, manganese oxides are more abundant in soils formed from mafic rocks than from siliceous clayey sediments (Dixon and White, 2002). Mn nodules are found in subsoil layers where the pH is higher than the upper layers, thus promoting Mn oxidation and precipitation of the oxides (Dixon and White, 2002). There is a general relationship between the type of Mn oxide and the age and maturity of the soil, birnessite occurs in young soils, todorokite occurs in young and intermediate-age soils and in rock weathering systems and litiophorite is the only one identified in nodules from old highly weathered soils (Dixon and White, 2002) (Figure 2.2).

Figure 2.2 Manganese oxide minerals formed in different environments (Dixon & White, 2002)

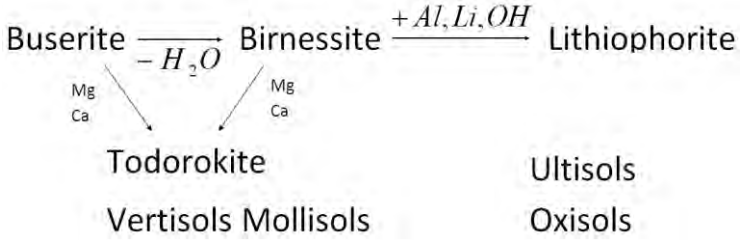

On the other hand, it has been reported that nodule formations is favored over concretion formation in silt loam texture soils that provide microsites for reoxidation of reduced Fe and Mn (D'Amore et. al., 2004). Concretions can form but may no longer be actively growing by accretion of iron and manganese if the source in the soil matrix has been exhausted (D'Amore et. al., 2004). Dixon and White (2002) reported that on shoulder slopes, Mn accumulation was greater at depths >1 m and much residual Mn persisted in unweathered silicate minerals. On footslopes Mn content was higher in the upper one-half meter of soil where it was correlated with a greater content of exchangeable ions, organic matter, and Mn removed by chemical fractionation.

Figure 2.3 Structure of soil lithiophorite and incorporation mechanism of nickel (Manceau et. al., 2002)

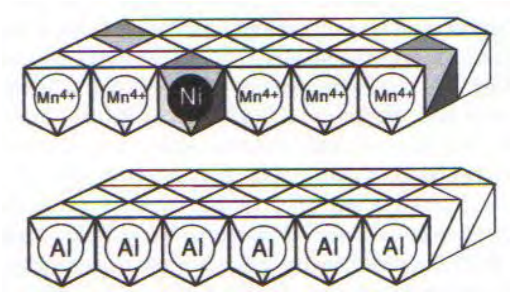

Manganese nodules have been also investigated in their structure and composition. Most Mn oxides exist in octahedral coordination surrounded by O atoms (Dixon and White, 2002). These are assembled by sharing edges or corners into a large variety of different structural arrangements, most of which fall into one of two major groups: (1) chain or tunnel structures, and (2) layers structures (Post, 1999). In the phyllomanganates, the octahedral have shared edges, and in the tectomanganates, the corners of the octahedral are shared to form tunnels (Dixon and White, 2002). Pyrolusite, ramsdellite, nsutite, hollandite, and todorokite are reported as tunnel structures and lithiophorite, chalcophanite, and birnessite are grouped as layer structures (Post, 1999). Because of the three different oxidation states of manganese (+2, +3, and +4), manganese oxides display a remarkable diversity of atomic architectures, many of which

easily accommodate a wide assortment of other metal cations (Post, 1999). Silicon, Fe, Al and Mn are being reported as the major elements of the iron-manganese nodules (Wen-Feng et. al., 2006). Also, the high reactivity of manganese oxides due to their high negative surface charge, low point zero charge and large surface area (Negra et. al., 2005a) makes them potential sites for ion fixation. These properties provide manganese oxides with high adsorption capacity and scavenging capability. Metals such as Ni, Zn, Co, Pb, Cd, Ba, and Ce are being reported to be sequestrated by ferromanganese nodules (Manceau et. al., 2003). For example, Manceau et. al. (2003) found that there is a systematic association of Ni with lithiophorite, suggesting that Ni should be located in a definite cation site of the manganese oxide crystal structure (Figure 2.3). Adsorption and precipitation of iron-manganese nodules could control the contents and chemical action of heavy metals in soil, and reduced activity of heavy metals in soil solution (Wen-Feng et. al., 2006). Understanding such processes is important for maintaining and improving soil fertility, mitigating health affects in humans and animals, and for treatment of water for consumption and industrial use (Post, 1999).

Manganese oxides are not only important sorbents for nutrients and pollutants, but also the catalysts for many chemical reactions, including redox reaction, which affects the concentration, species, chemical behavior, availability, and toxicity of trace metals to plants and animals in soil and sediments (Wen-Feng et. al, 2006; Adams *et al.*, 1969; Gilkes, 1988; Huang, 1991; Murray and Dillard, 1979). Their oxidation potentials are even higher than O_2 (Dixon and White, 2002). Manganese oxides can oxidize Co^{2+} to Co^{3+}, Cr^{3+} to Cr^{6+}, and As^{3+} to As^{5+}. In particular, Mn is the only known oxidizer of trivalent Cr in soils (Negra et. al., 2005a).

Techniques such as transmission electron microscopy, x-ray powder diffraction (Figure 2.4), infrared spectroscopy, and x-ray absorption spectroscopy have made it possible to partially solve and refine structures of manganese oxides minerals.

Figure 2.4 X-ray diffraction patterns for birnessite, todorokite, and lithiophorite (Dixon & White, 2002)

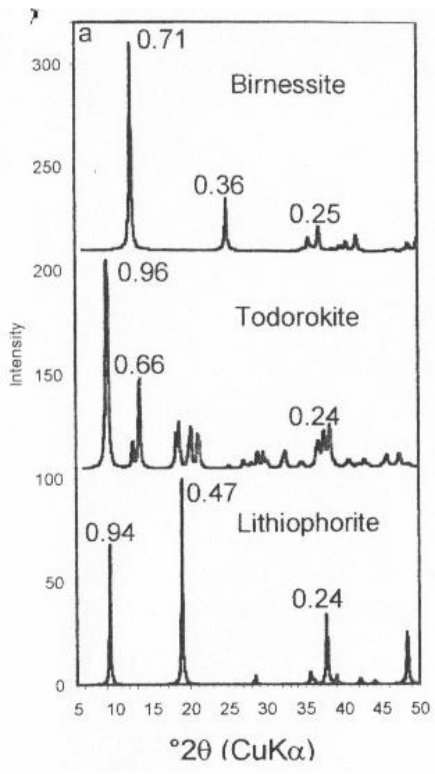

3 Evaluation and Characterization of the Soil Profiles

3.1 Methodology

Three pits with different elevations were dug at the Coloso Valley Agricultural Reserve located in western Puerto Rico. Each soil profile was described using the *Field Book for Describing and Sampling Soils* from Natural Resources Conservation Services as a reference. Physical properties such as horizon presence and width, color, rocks, structure, consistence, redoximorphic features, concentration, ped and void surface features, roots, and pores were evaluated. Texture and pH were estimated in the field by hand and using the *Hellige-Truog Soil Reaction Tester*, respectively. Manganese masses, nodules or concretions were tested in the field with a solution of 3% hydrogen peroxide (H_2O_2). During this field test manganese dioxide catalyses the decomposition of hydrogen peroxide to oxygen and water:

Figure 3.1 Field pH Determination Using the Hellige-Truog Soil Reaction Tester

$$2H_2O_2 \xrightarrow{MnO_2} O_2 + 2H_2O.$$

Figure 3.2 Effervescent reaction during manganese features test

After the field description, soil samples were collected, air-dried, ground to pass through a 2-mm sieve and stored in plastic bags. The physical and chemical properties of the samples were analyzed or corroborated in the laboratory. Texture was corroborated in the laboratory quantitatively

by the hydrometer method and pH was corroborated using a 2:1 water:soil ratio using a model 310 ORION perpHect LogRmeter.

We determined the taxonomic class of the soil profiles using the data collected from the field, chemical properties, the *Keys to Soil Taxonomy* from USDA-NRCS and a report with recommendations from the USDA-NRCS Major Land Resource Area Leader (Appendix C) as reference. The classes calculated of each soil were particle-size, mineralogy, cation-exchange activity and soil temperature.

3.2 Results and Discussion

3.2.1 Site Description

The Coloso Valley Agricultural Reserve is located in northwest Puerto Rico in the municipality of Aguada. The soils of the Coloso Valley are surrounded by the Cañas and Culebrinas Rivers (Appendix A). The Culebrinas River originates in southwestern Lares municipality and flows for 25 miles until it empties into the Mona Passage between Aguada and Aguadilla municipalities. It passes through several geological formations from Upper Cretaceous, Younger Tertiaries (Aguada Limestone and San Sebastian Formation) and Igneous Lava Flows dissolving and bringing a mixed parent material to the valley. The toposequence starts with Rio Piedras pedon in the south part of the Valley at 18˚ 22’ 47.1’’N 67˚ 08’ 57.2’’W. Next is the Bajura pedon at 800 meters north from Rio Piedras site at 18˚ 23’ 13.5’’N 67˚ 09’ 00.7’’W and 500 meters north from Bajura is Coloso pedon at 18˚ 23’ 29.9’’N 67˚ 08’ 58.1’’W.

3.2.2 Pedons Descriptions

The soils profiles were identified in the Web Soil Survey from Natural Resources Conservation Services as Rio Piedras (Typic Hapludults), Bajura (Vertic Endoaquolls), and Coloso (Vertic Dystrudepts) (See Appendix B). Rio Piedras soil occurs at high elevations (~20m). Coloso and Bajura soils occur at the lower levels (~5m). The Rio Piedras pedon had 8 horizons. They were identified in the field as: One Ap (0 to 20 centimeters), three Bts (20 to 36, 36 to 53, and 53 to 69 centimeters), three Btvs (69 to 104, 104 to 135, and 135 to 163 centimeters), and one C (more than 163 centimeters) (Figure 3.3). Yellow-Red colors were dominant in the horizons and texture was clay loam throughout. Manganese concretions were found in the Ap horizon and manganese masses in the Bt_1. Plinthite nodules were found in the Bt_2, Bt_3 and Btv horizons. Soil pH was strongly acid throughout the whole profile. Bajura pedon had 5 horizons. One Ap (0 to 20 centimeters), one A (20 – 38 centimeters), two Bwg (38 to 58 and 58 to 86 centimeters), and one Cg (86 – 160 centimeters) were identified in the field (Figure 3.4). Grayish brown colors were dominant in the horizons and texture was clay throughout. Manganese masses were found in the A, Bwg_1 and Cg horizon and manganese concretions in the Bwg_2. Soil pH was slightly alkaline in the Ap, A and Bwg_1 and neutral in the Bwg_2 and Cg horizons. Coloso pedon had 5 horizons: one Ap (0 to 36 centimeters), one Bw (36 – 58 centimeters), two Btg (58 to 89 and 89 to 117 centimeters), and one Bwg (117 – 165 centimeters) (Figure 3.5). Brown colors were dominant in the horizons and texture was clay throughout. Manganese concretions were found in the Btg_2 and Bwg horizons and manganese masses in the Bw. Soil pH was moderately alkaline throughout using the *Hellige-Truog Soil Reaction Tester*.

3.2.3 Pedons Samples Chemical Analysis

Rio Piedras pedon resulted extremely acid throughout with pH values from 3.6 to 4.4. The first two horizons of Bajura soil were slightly acid and last three horizons were neutral. The first three horizons of Coloso soil were slightly alkaline and the last two horizons were neutral. The pH of Rio Piedras and Bajura pedons increased with increasing depth, while in Coloso the pH decreased with depth (Table 3.4). Texture of all the horizons of the three soil profiles were clay throughout (Table 3.5).

Figure 3.3 Rio Piedras Pedon

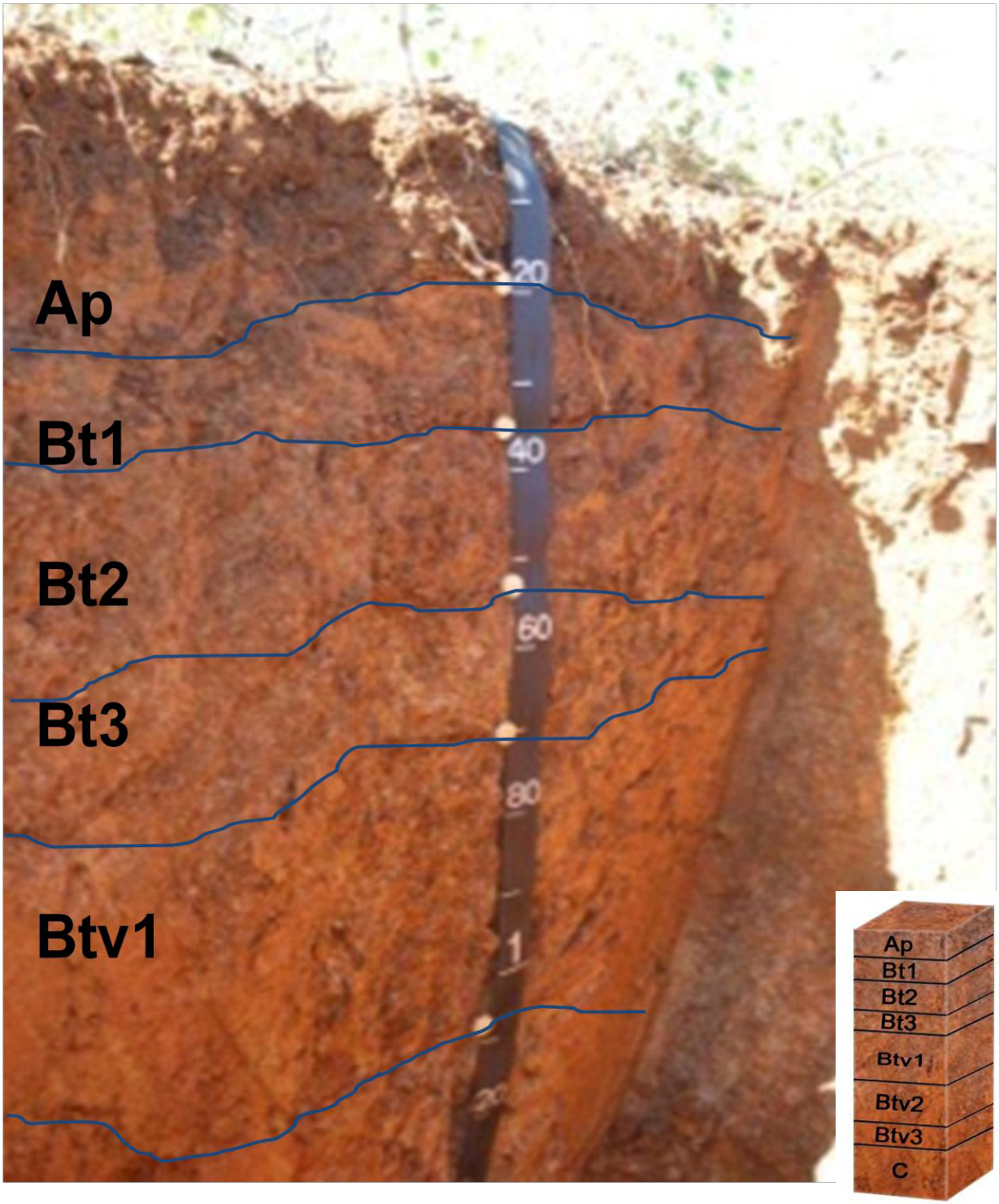

Figure 3.4 Bajura Pedon

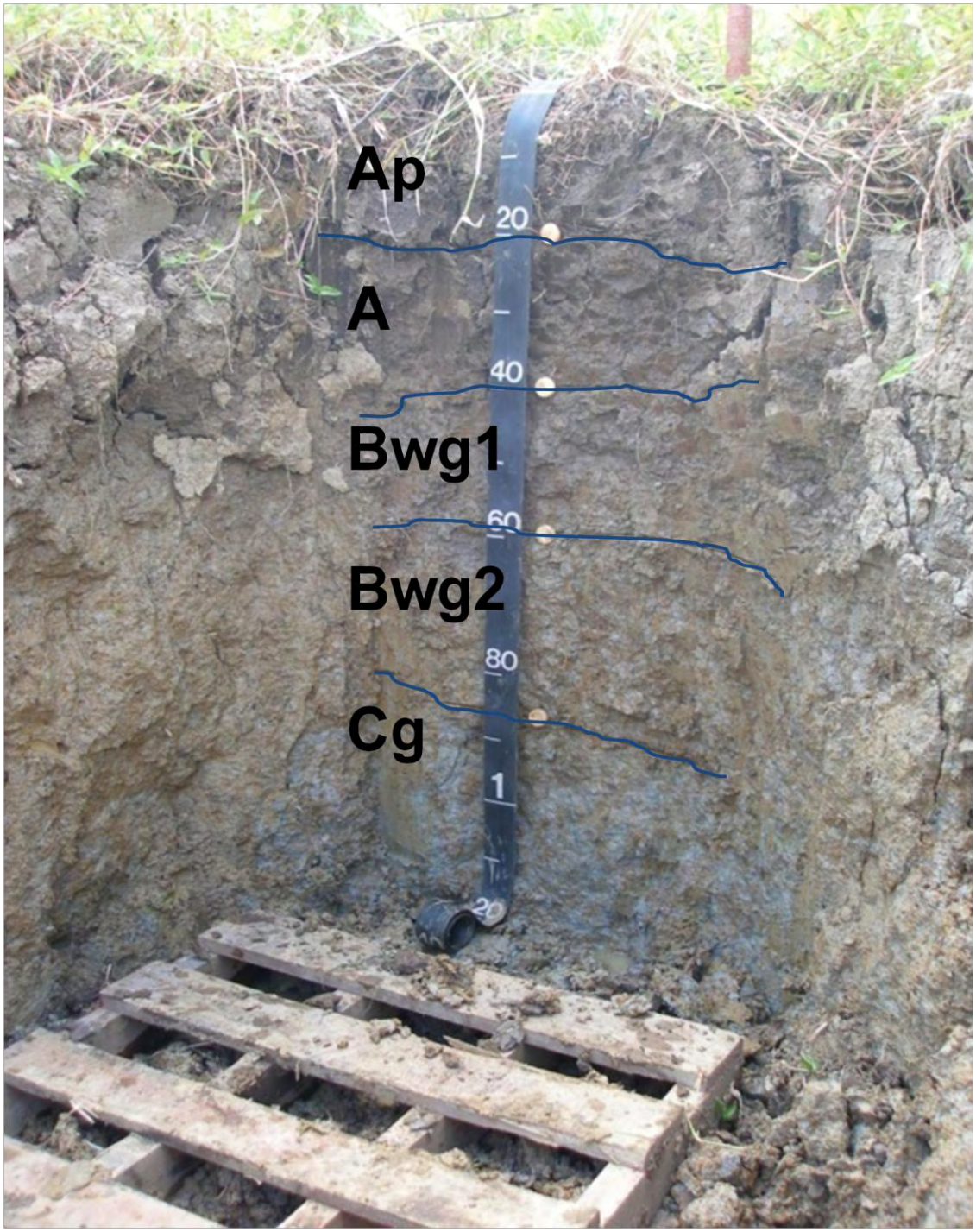

Figure 3.5 Coloso Pedon

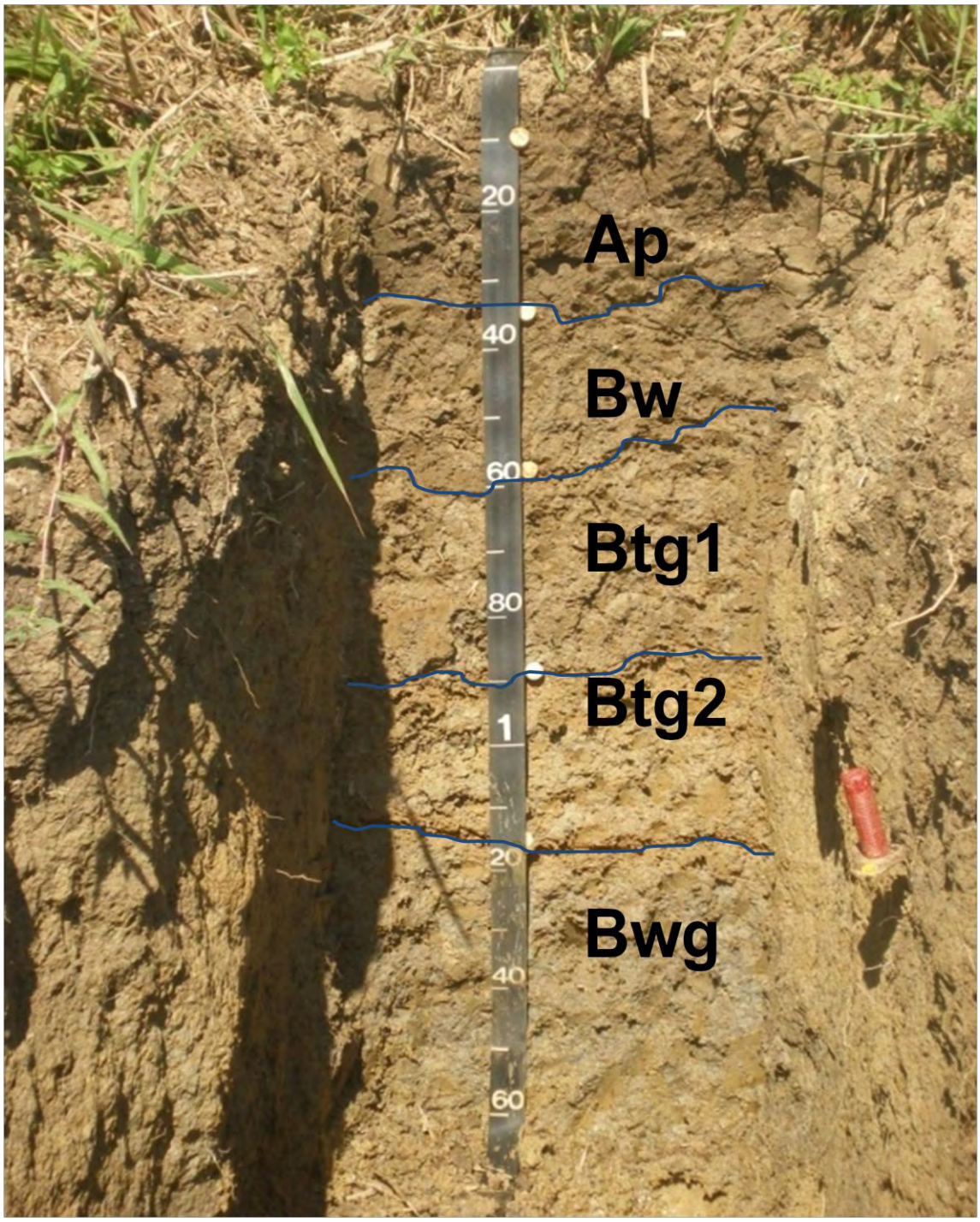

Table 3.1 Rio Piedras Field Pedon Description

	Horizon	Depth (cm)	Color (moist)	Texture	Concentrations	Redoximorphic Features	pH
1	Ap	0 – 20	5YR 4/4	CL	15%, Fe-Mn concretions		4.5
2	Bt_1	20 – 36	60% 7.5YR 5/6 40% 2.5YR 4/6	CL	10%, Fe-Mn concretions 10YR 2/1		4.5
3	Bt_2	36 – 53	80% 7.5YR 5/6 20% 10YR 8/1	CL	10%, Fe masses 2.5YR 4/6	<2%, PLN 10R 4/8	4.5
4	Bt_3	53 – 69	60% 7.5YR 5/6 20% 5YR 5/6 20% 10YR 8/1	CL		<5%, PLN 10R 4/8	5.0
5	Btv_1	69 – 104	40% 2.5YR 4/6 40% 10YR 6/6 10% 10YR 8/1 10% 10YR 7/8	CL		~15%, PLN 10R 4/8	5.0
6	Btv_2	104 – 135	10YR 6/3	CL	~15%, Fe masses 2.5YR 5/8 ~2%, Fe masses 7.5YR 6/8	~10%, PLN 10R 4/8	4.5
7	Btv_3	135 – 163	5Y 7/3	CL	~3%, Fe masses 10YR 6/8	~5%, PLN 10R 4/8	4.5
8	C	163 +	5Y 7/3	CL	~10%, Fe masses 10YR 6/8		4.5

Table 3.2 Bajura Field Pedon Description

	Horizon	Depth (cm)	Color (moist)	Texture	Concentrations	Redoximorphic Features	pH
1	Ap	0 – 20	80% 710YR 3/2 20% 10YR 3/1	C		c,f, 10YR 4/6 oxidation root channel	7.5
2	Bt_1	20 – 38	80% 10YR 3/1 20% 10YR 3/2	C	15%, Fe masses 10YR 5/6 5%, Fe-Mn masses	c,f, 10YR 4/6 oxidation root channel	7.5
3	Bt_2	38 – 58	60% 10YR 5/1 40% 10YR 5/6	C	10%, Fe-Mn masses 5%, Fe masses 5YR 4/6	10YR 4/1 depleted root channel	7.5
4	Bt_3	58 – 86	75% 10YR 5/1 25% 10YR 4/6	C	10%, Fe-Mn concretions 5%, Fe-Mn masses 7.5YR 5/8	10YR 3/1 depleted root channel	7.0
5	Btv_1	86 – 160	70% 5GY 5/1 30% 7.5YR 5/8	C	5%, Fe-Mn masses (+H2O2)		7.0

Table 3.3 Coloso Field Pedon Description

	Horizon	Depth (cm)	Color (moist)	Texture	Concentrations	Redoximorphic Features	pH
1	Ap	0 – 36	10YR 4/1	C	Fe masses 7.5YR 4/4		8.0
2	Bt_1	36 – 58	70% 10YR 5/1 30% 10YR 5/8	CL	10%, Fe masses 5YR 4/4 5% Fe-Mn masses		8.0
3	Bt_2	58 – 89	90% 10YR 5/1 10% 10YR 4/6	C	~10%, Fe-Mn concretions 15% Fe masses 7.5YR 4/6		8.0
4	Bt_3	89 – 117	65% 10YR 5/6 35% 10YR 5/6	CL	5% Fe-Mn concretions		8.0
5	Btv_1	117 – 165	80% 10YR 4/1 20% 10YR 4/6	C			8.0

Table 3.4 Determination of the Horizons' pH Using a 2:1 water:soil ratio

Rio Piedras			
	Horizon	Depth (cm)	pH
1	Ap	0 – 20	3.6
2	Bt1	20 – 36	3.8
3	Bt2	36 – 53	3.9
4	Bt3	53 – 69	3.9
5	Btv1	69 – 104	3.9
6	Btv2	104 – 135	4.0
7	Btv3	135 – 163	4.3
8	C	163 +	4.4

Bajura			
	Horizon	Depth (cm)	pH
1	Ap	0 – 20	6.4
2	A	20 – 38	6.5
3	Bwg1	38 – 58	6.7
4	Bwg2	58 – 86	6.8
5	Cg	86 – 160	6.9

Coloso			
	Horizon	Depth (cm)	pH
1	Ap	0 – 36	7.4
2	Bw	36 – 58	7.5
3	Btg1	58 – 89	7.4
4	Btg2	89 – 117	7.2
5	Bwg	117 – 165	7.2

Table 3.5 Determination of the Horizons' Texture Using the Hydrometer Method

	Rio Piedras					
	Horizon	Depth (cm)	Sand Percent	Silt Percent	Clay Percent	Texture
1	Ap	0 – 20	0.21	0.11	0.67	Clay
2	Bt_1	20 – 36	0.20	0.10	0.70	Clay
3	Bt_2	36 – 53	0.18	0.15	0.68	Clay
4	Bt_3	53 – 69	0.12	0.16	0.72	Clay
5	Btv_1	69 – 104	0.15	0.17	0.68	Clay
6	Btv_2	104 – 135	0.12	0.13	0.74	Clay
7	Btv_3	135 – 163	0.14	0.12	0.73	Clay
8	C	163 +	0.15	0.10	0.75	Clay

	Bajura					
	Horizon	Depth (cm)	Sand Percent	Silt Percent	Clay Percent	Texture
1	Ap	0 – 20	0.13	0.22	0.65	Clay
2	A	20 – 38	0.11	0.20	0.70	Clay
3	Bwg_1	38 – 58	0.10	0.17	0.73	Clay
4	Bwg_2	58 – 86	0.11	0.18	0.71	Clay
5	Cg	86 – 160	0.13	0.18	0.69	Clay

Table 3.5 Determination of the Horizons' Texture Using the Hydrometer Method (cont.)

	Coloso					
	Horizon	Depth (cm)	Sand Percent	Silt Percent	Clay Percent	Texture
1	Ap	0 – 36	0.12	0.21	0.67	Clay
2	Bw	36 – 58	0.19	0.21	0.60	Clay
3	Btg_1	58 – 89	0.11	0.20	0.69	Clay
4	Btg_2	89 – 117	0.14	0.20	0.66	Clay
5	Bwg	117 – 165	0.15	0.19	0.65	Clay

3.2.4 Pedons Characterizations

The clay percent in the control section of Rio Piedras pedon was 69.07%, Bajura's pedon was 70.97% and Coloso's 65.53%. The three pedons are classified as very fine. Thermal analysis data provided by USDA-NRCS indicate that mineralogy in the control section was 57% kaolinitic and 4% gibbsite for Rio Piedras and 63% kaolinitic and 5% gibbsite for Bajura. The soil temperature in this area is isohyperthermic (above 22˚ C) and the difference between the mean summer and the mean winter soil is 6˚ C or less (Lugo-Camacho, 2005). The soil moisture regime is udic. According to these results, the data collected from field observations and recommended by USDA-NRCS MLRA 15 – 9 Soil Survey Office, Rio Piedras' pedon classifies as Very fine, kaolinitic, isohyperthermic Oxic Dystrudepts, Bajura's pedon as Very fine, kaolinitic, isohyperthermic Fluventic Edoaquepts and Coloso as Very fine, kaolinitic, isohyperthermic Vertic Endoaquepts.

Table 3.6 Particle-size class determination in Rio Piedras pedon

Former Horizon Designation	Thickness (in)	Clay Percent	Thickness * Clay %	Total thickness * Total Clay %
Bt_1	4	70	280	
Bt_2	7	68	476	
Bt_3	6	72	432	
Btv_1	13	68	884	
Total	30		2072	69.07

Table 3.7 Particle-size class determination in Bajura pedon

Former Horizon Designation	Current Horizon Designation	Thickness (in)	Clay Percent	Thicknes * Clay %	Total thickness * Total Clay %
A	AB	5	70	350	
Bwg_1	Bwg_1	8	73	584	
Bwg_2	Bwg_2	11	71	781	
Cg	Cg	6	69	414	
Total		30		2129	70.97

Table 3.8 Particle-size class determination in Coloso pedon

Former Horizon Designation	Current Horizon Designation	Thickness (in)	Clay Percent	Thicknes * Clay %	Total thickness * Total Clay %
Ap	Ap	4	67	268	
Bw	Bw	9	60	540	
Btg_1	Bwg_1	12	69	828	
Btg_2	Bwg_2	5	66	330	
Total		30		1966	65.53

4 Quantification and Characterization of Manganese Nodules

4.1 Methodology

A subsample of 800 g from each soil horizon was washed with distilled water using a # 10 sieve to extract manganese nodules greater than 2 mm (Figure 4.1). Manganese nodules were placed in a desiccator for 48 hours, weighed and evaluated for concentric layering using an Olympus SZX – 12 Stereomicroscope, Paxit Digital Camera and Imaging Software. The nodules were ground using an agate mortar and then analyzed by x-ray diffraction using a Siemens D-5000 Diffraktometer.

Figure 4.1 Manganese Nodules Extraction.

4.2 Results and Discussion

Manganese nodules from each soil differ in occurrence, kind, size, quantity and position. The largest Mn nodules were observed in the Ap horizon of the Rio Piedras soil series; however this site had the fewest nodules. Two grams of manganese nodules per 800 g of soil were observed. In Bajura and Coloso soil series, the largest occurrence of manganese nodules was observed in the Bwg horizon. The nodule mass in Bajura soil was 11 g/800 g and in Coloso soil

Figure 4.2 Manganese masses in Bajura Soil Profile.

it was 15 g/800 g (Table 4.1). Manganese nodules from the Rio Piedras soil were well formed with clearly defined concentric layers (Figure 4.4). In the Coloso and Bajura soils the Mn nodules were not well formed and irregular masses of Mn oxides were observed on soil peds (Figure 4.2). In Bajura and Coloso, as depth increases, the mass of manganese nodules also increase until they hit the horizon with permanent saturating conditions. In Rio Piedras as depth increases, the mass of manganese nodules decreases and only the Ap horizon presents a significant amount of manganese nodules.

X-ray diffraction patterns of all the manganese nodules were very similar with broader peaks. The presence of quartz is indicated by a narrow peak around 26.5˚ 2-Theta. Peaks around 10 – 14 and 35 – 40˚ 2-Theta indicated the possible presence of lithiophorite or todorokite. We suggest that peaks around 19 – 21˚ are todorokite and at 50˚ are lithiophorite (Figures 4.4-4.8).

Figure 4.3 Manganese modules images using an Olympus SZX – 12 Stereomicroscope, Paxit Digital Camera and Imaging Software. Up: Mn nodules from Rio Piedras Soil Series, Close up of first image showing concentric layers. Down: Bajura Soil Series concretions and Close up of concretions showing the absence of concentric layers.

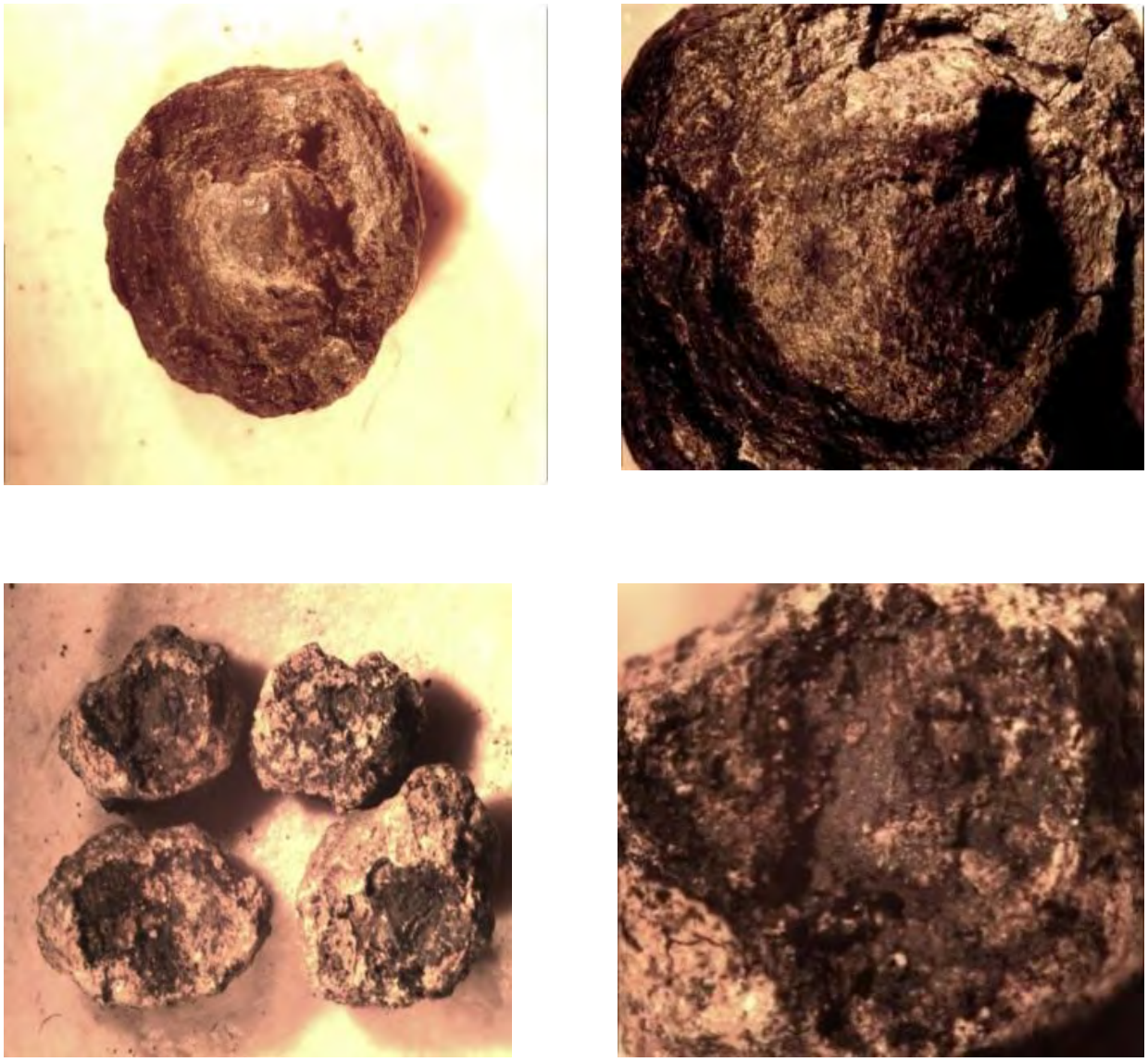

Table 4.1 Quantification of Manganese Nodules

	Rio Piedras			
	Horizon	Depth (cm)	Weight (g)	Percent
1	Ap	0 – 20	2.0349	0.25
2	Bt_1	20 – 36	0.5919	0.07
3	Bt_2	36 – 53	0.4346	0.05
4	Bt_3	53 – 69	0.0677	0.01
5	Btv_1	69 – 104	0.0672	0.01
6	Btv_2	104 – 135	0	0
7	Btv_3	135 – 163	0	0
8	C	163>	0	0

	Bajura			
	Horizon	Depth (cm)	Weight (g)	Percent
1	Ap	0 – 20	0	0
2	A	20 – 38	0.1994	0.02
3	Bwg_1	38 – 58	0.9393	0.12
4	Bwg_2	58 – 86	9.7367	1.22
5	Cg	86 – 160	2.4449	0.31

	Coloso			
	Horizon	Depth (cm)	Weight (g)	Percent
1	Ap	0 – 36	0	0
2	Bw	36 – 58	0.1632	0.02
3	Btg_1	58 – 89	1.1624	0.15
4	Btg_2	89 – 117	12.9529	1.62
5	Bwg	117 – 165	14.9704	1.87

Figure 44 X-ray diffraction patterns of manganese nodules of Rio Piedras' Ap horizon

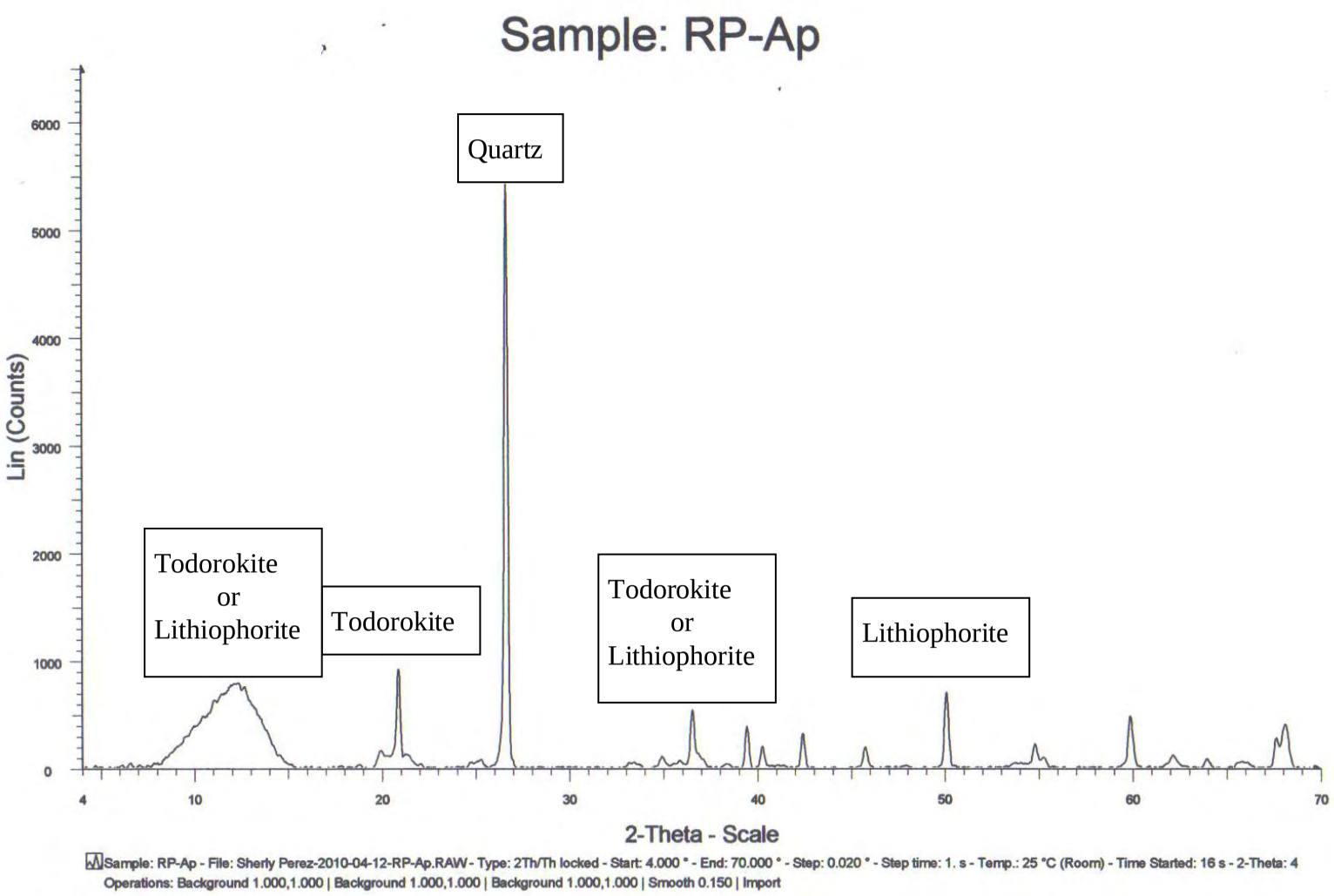

Figure 4.5 X-ray diffraction patterns of manganese nodules of Bajura's Bwg2 horizon

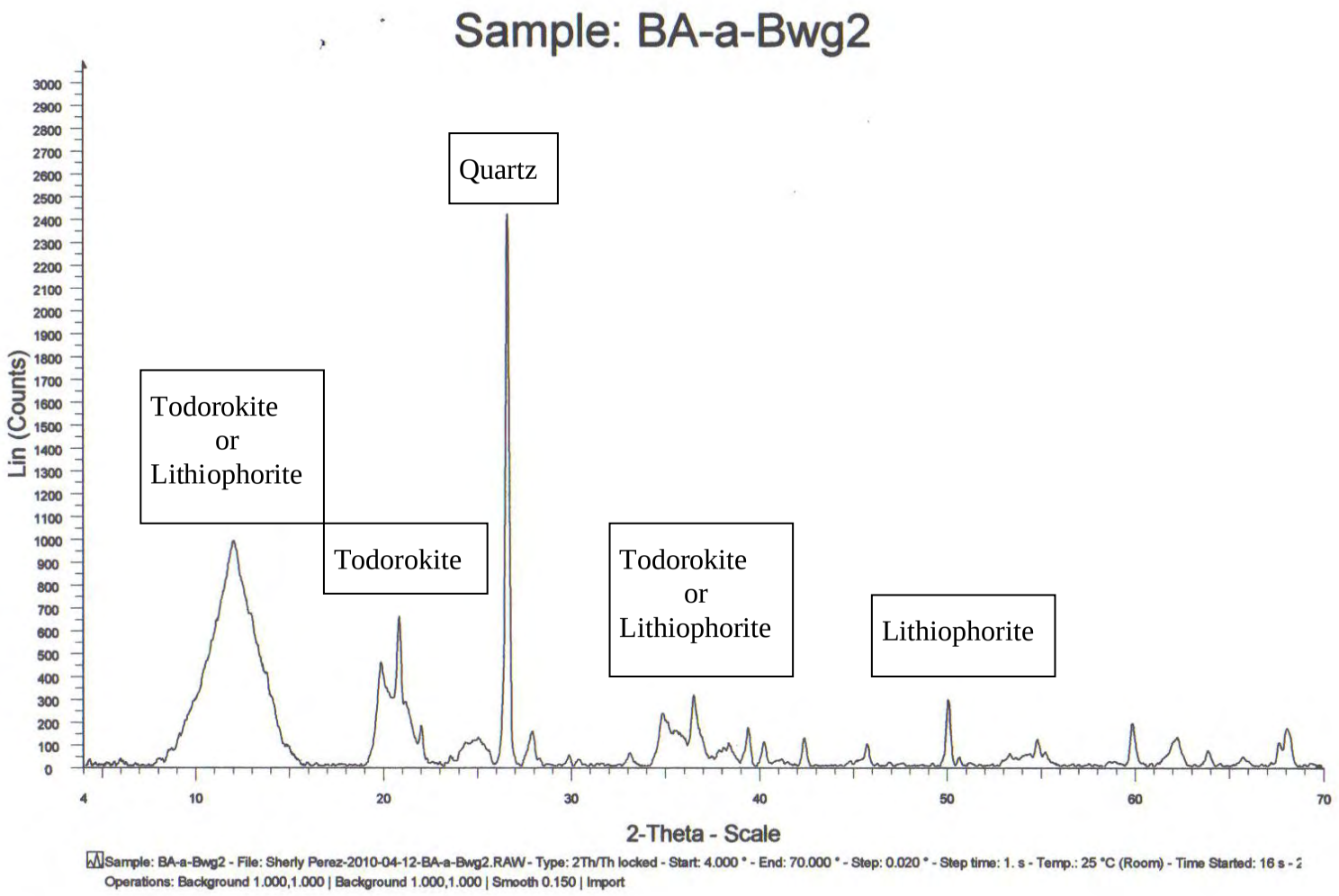

Figure 4.6 X-ray diffraction patterns of manganese nodules of Bajura's Cg horizon

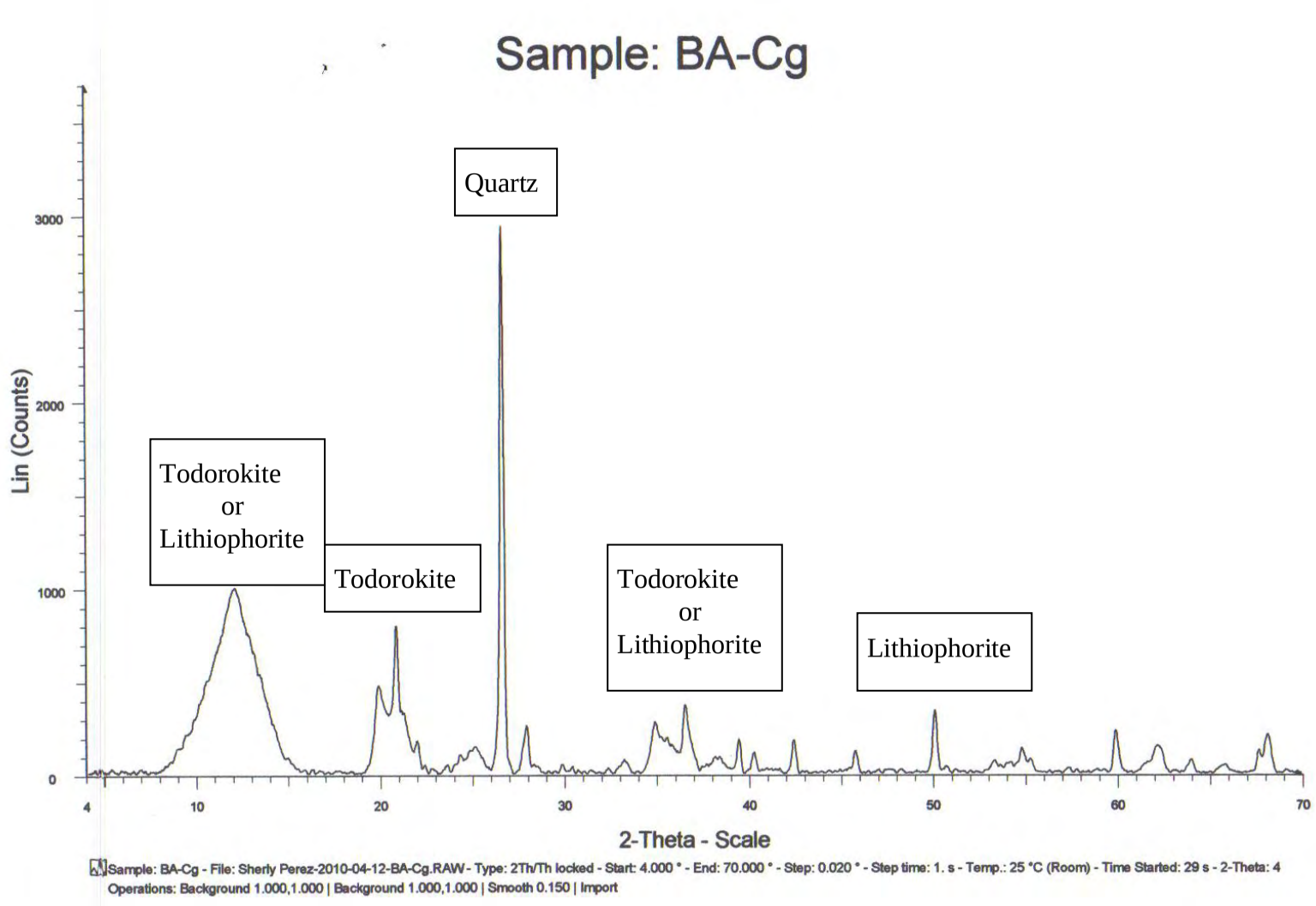

Figure 4.7 X-ray diffraction patterns of manganese nodules of Coloso's Btg2 horizon

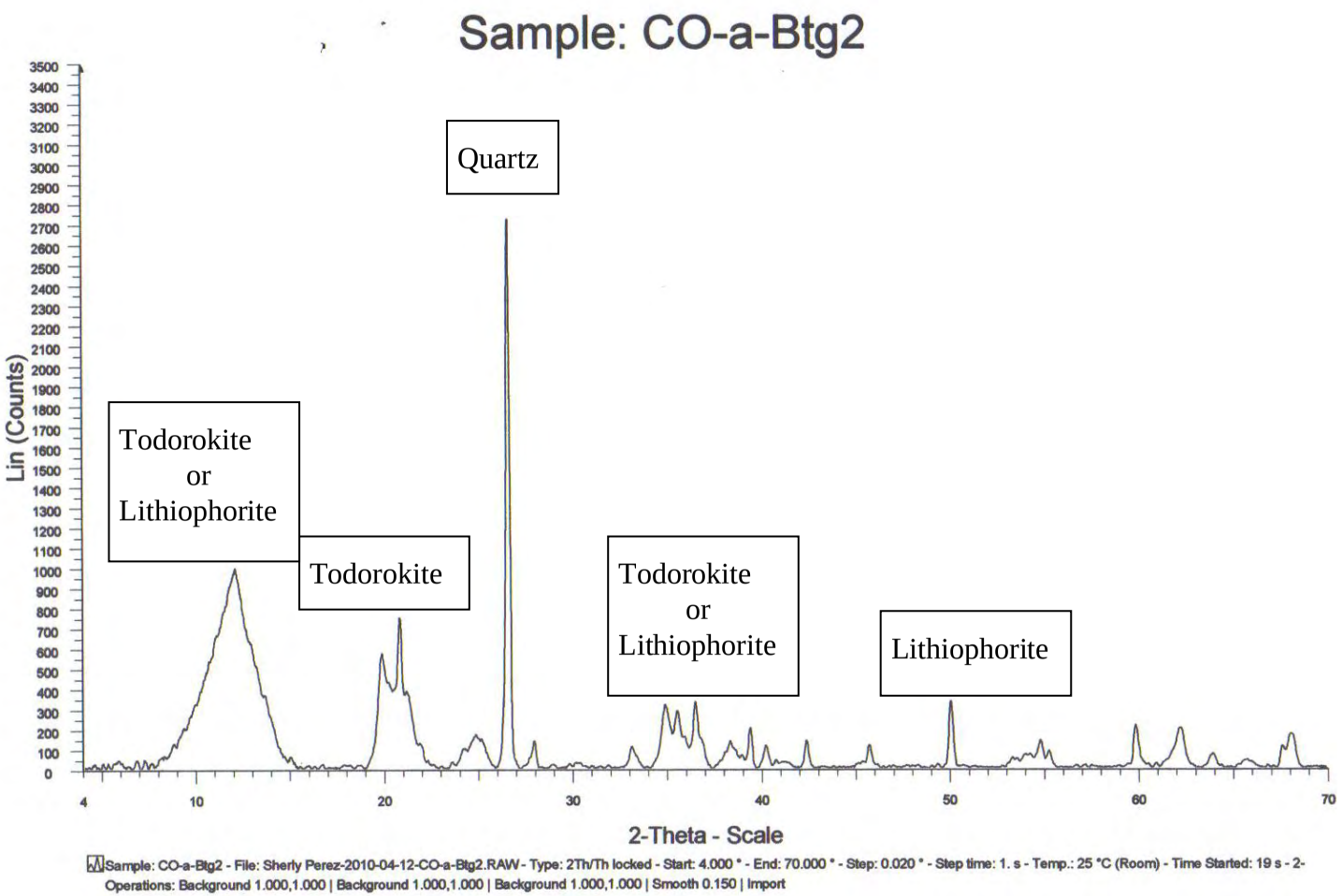

Figure 4.8 X-ray diffraction patterns of manganese nodules of Coloso's Bwg horizon

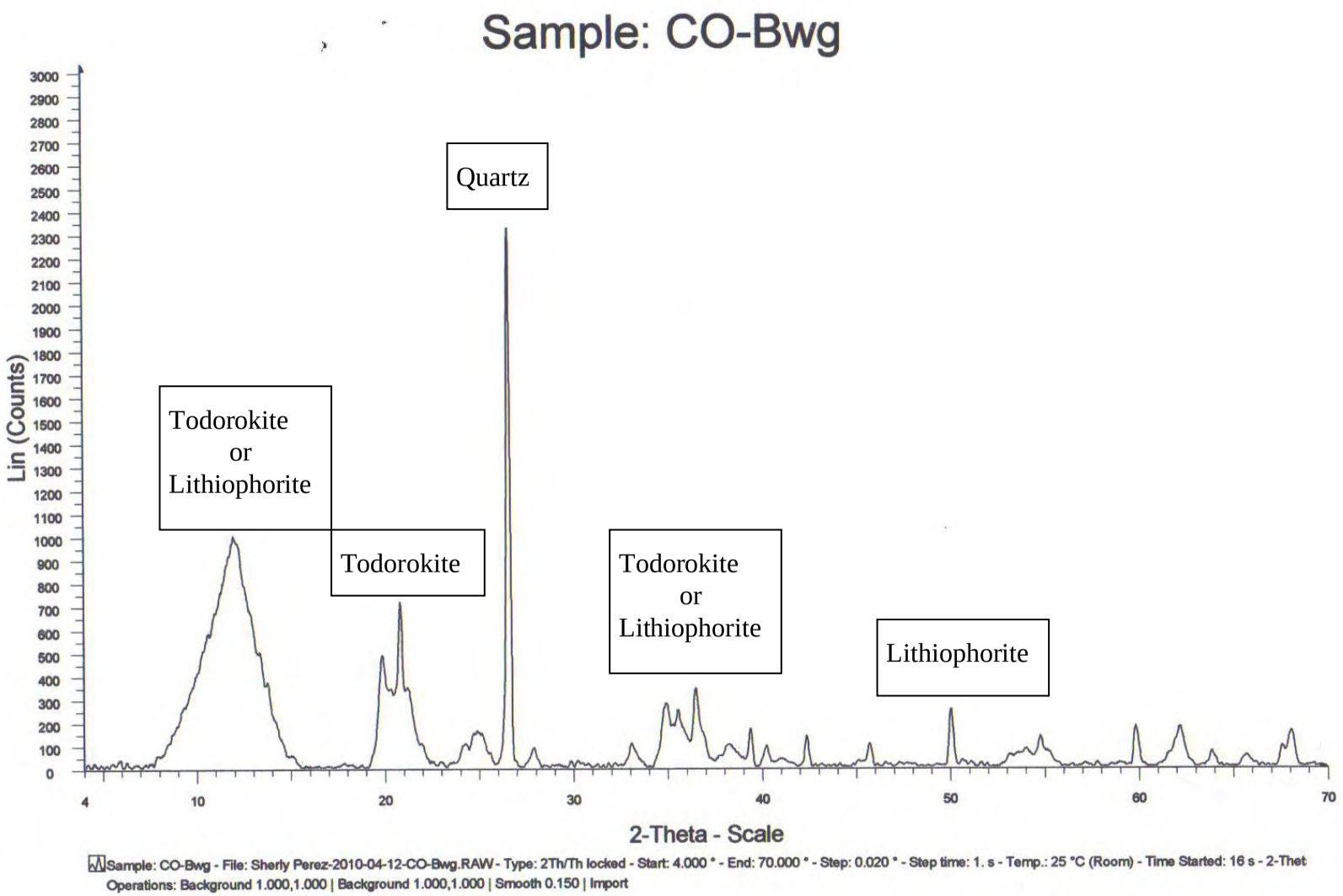

5 Conclusions

We proposed that the occurrence of manganese redoximorphic features in the Coloso Valley Agricultural Reserve is influenced by hydrology and geology. The soils of the Coloso Valley are surrounded by the Cañas and Culebrinas Rivers (Appendix A) which causes the variability in the water table and brings a variety of elements such as manganese to the valley. We proposed that the variability in occurrence, size and shape of manganese nodules are also influenced by the topography of the site. Coloso and Bajura pedons occur at the lower levels in the toposequence, where they are subjected to continuing soil depositon (nutrients) and to wetting and drying. In Bajura and Coloso pedons a more active redox process of Mn is taking place. This process results in the formation of small manganese nodules and masses, but greatest in occurrence. Rio Piedras pedon occurs at higher elevation and the water table never saturates the soil profile. The lack of soil environment for concretion formation explains the fewest occurrences. To explain the occurrence of manganese nodules we proposed the theory that Rio Piedras pedon once was at the same elevation of Bajura and Coloso and a significant geologic change, for example an event of soil uplifting brought the soil to a higher elevation. Then, the highest rate of oxidation creates stability and well formed nodules. Although a clear differentiation between lithiophorite and todorokite was not possible by XRD we should expect a predominance of lithiophorite in the older soil. A total chemical analysis of nodules composition may be helpful to differentiate between both oxides, since Al and Li are two components of lithiophorite.

6 References

Adams, S.N., J.L. Honeysett, K.G. Tiller and K. Norrish. 1969. Factors controlling the increase of cobalt in plants following the addition of cobalt fertilizer. Aust. J. Soil Res. 7: 29 – 42.

Beinroth, F.H., R.J. Engel, J.L. Lugo, C. L. Santiago, S. Rios and G.R. Brannon. 2003. Updated taxonomic classification of the soils of Puerto Rico, 2002. Bulletin 302, Agric. Expt. Station, Univ. P.R., Mayaguez Campus.

Burns, R.G. 1976. The uptake of cobalt into ferromanganese nodules, soils, and synthetic manganese (IV) oxides. Geochimica et Cosmochimica Acta. 40: 95 – 102.

Burns, R.G. and V.M. Burns. 1975. Mechanism for nucleation and growth of manganese nodules. Nature (London). 255: 130 – 131.

D'Amore, D. V., S. R. Steward, and J. Herbert. 2004. Saturation, Reduction, and the Formation of Iron-Manganese Concretions in the Jackson-Frazier Wetland, Oregon. Soil Sci. Soc. Am. J. 68: 1012 – 1022.

Dixon, F. B, and G. Norman White. 2002. Soil Mineralogy with Environmental Applications. SSSA Book Series, no. 7. 367 p.

Dixon, F. B, and H. C. W. Skinner. 1992. Manganese minerals in surface environments. *In* Skinner, H. C. W. and R. W. Fitspatrick. Biomineralisation Processes of Iron and Manganese-Modern and Ancient Environments. Cremlingen, Germany. 31-50 p.

Gambrell, R. P. 1996. Manganese. Methods of Soil Analysis. Part 3. Soil Science Society of America and American Society of Agronomy. Wisconsin, USA.

Gilkes, R. J. 1988. Geochemistry and mineralogy of manganese in soils. *In* Graham, R.D. and K.J. Hannam. Manganese in Soils and Plants. Kluwer Academic publishers, Netherlands. pp. 23 – 35.

Gon, J, J. B. Dixon, C. C. Chusuei, and Y. Deng. 2002. Oxidation of Chromium (III) to (IV) by Manganese Oxides. Soil Sci. Soc. Am. J. 66: 306 – 315.

Hem, J.D. 1963. Chemical Equilibria Affecting the Behavior of Manganese in Natural Water. Hydrological Sciences Journal, 8:3, 30 – 37.

Huang, P.M. 1991. Kinetics of redox reactions on manganese oxides and its impact on environmental quality. *In* Sparks, D.L. and D.L. Suarez. Rate of Soil Chemical processes. SSSA Spec. Publ. 27. SSSA, Madison, WI, USA.

Kim, J.G., J.B. Dixon and Y. Deng. 2002. Oxidation of Chromium (III) to (VI) by Manganese Oxides. Soil Sci. Soc. Am. J. 66: 306 – 315.

Liu, F., C. Colombo, P. Adamo, J.Z. He and A. Violante. 2002. Trace Elements in Manganese-Iron Nodules from a Chinese Alfisol. Soil Sci. Soc. Am. J. 66: 661 – 670.

Lugo-Camacho, J.L. 2005. The Soil Climate Regimes of Puerto Rico-Reassessment and Impliations. M.S. Thesis. Department of Agronomy and Soil Science, University of Puerto Rico-Mayagüez.

Manceau, A., N. Tamura, M. A. Marcus, A. A. MacDowell, R. S. Celestre, R. E. Sublett, G. Sposito, and H. A. Padmore. 2002. Deciphering Ni sequestration in soil ferromanganese nodules by combining X – ray fluorescence, absorption, and diffraction at micrometer scales of resolution. American Mineralogist. 87: 1494 – 1499.

Manceau, A., N. Tamura, R. S. Celestre, A. A. Macdowell, N. Geoffroy, G, Sposito, and H. A. Padmore. 2003. Molecular – Scale Speciation of Zn and Ni in soil Ferromanganese Nodules from Loess Soils of the Mississippi Basin, Environ. Sci, Technol. 37: 75 – 80.

McKenzie, R. M. 1989. Manganese oxides and hydroxides. *In* Dixon, J. B. and S. B., Weed. Minerals in Soil Environments. SSSA Book, no. 1. 439-465 p.

Murray, J.W. and J.G., Dillard. 1979. The oxidation of cobalt (II) adsorbed on manganese dioxide. Geochim. Cosmochim Acta. 43: 781 – 787.

Negra, C., D. S. Ross, and A. Lanzirotti. 2005a. Oxidizing Begavior of Soil Manganese: Interactions among Abundance, Oxidation State, and pH. Soil Sci. Soc. Am. J. 69: 87 – 95.

Negra, C., D. S. Ross, and A. Lanzirotti. 2005b. Soil Manganese Oxides and Trace Metals: Competitive Sorption and Microfocused Synchrotron X – ray Fluorescence Mapping. Soil Sci. Soc. Am. J. 69: 353 – 361.

Post, J. E. 1999. Manganese oxide minerals: Crystal structures and economic and environmental significance. Proc. Natl. Acad. Sci. 96: 3447-3454.

Rhoton, F.E., J.M. Bigham, D.G. Shulze. 1993. Properties of Iron-Manganese Nodules from a Sequence of Eroded Fragipan Soils. Soil Sci. Soc. Am. J. 57: 1386 – 1392.

Schaetzl, R. and S. Anderson. 2005. Soils: genesis and geomorphology. University Press, Cambridge.

Schoeneberger, P.J., D.A. Wysocki, E.C. Benham and W.D. Broderson. 2002. Field book for describing and sampling soils, Version 2.0. Natural Resources Conservation Services, National Soil Survey Center, Lincoln, NE.

Shih-Hao J. and Zueng-Sang C. 2006. Characterization and Formation of Iron-Manganese Nodules of Ultison with Plinthite in Taiwan. 18th World Congress of Soil Science.

Sullivan, L. A. and A.J.,Koppi. 1992. Manganese oxide accumulations associated with some soil structural pores: I. Morphology, composition and genesis. Aust. J. Soil Res. 30: 409 – 427.

Taiz, L. and E. Zeiger. 2002. Plant Physiology. 3rd ed. Sinauer Associates, Inc.

Tebo, B. M. and L. M., He. 1998. *In* Sparks, D. L. and T.J. Grundl. 1998. Mineral-Water Interfacial Reactions: Kinetics and Mechanisms. American Chemical Society: Washington, DC. 393-414 p.

United States Department of Agriculture, Natural Resources Conservation Services. 2010. Field Indicators of Hydric Soils in the United States. A Guide for Identifying and Delineating Hydric Soils. Version 7.0. Vasilas, L.M., G.W. Hurt and C.V. Noble (eds.).

Uzochukwu, G.A. and J.B. Dixon. Manganese Oxide Minerals in Nodules of Two Soils of Texas and Alabama. 1986. Soil Sci. Soc. Am. J. 50: 1358 – 1363.

Wen-Feng, T., L. Fan, L. Yong-Hua, H. Hong-Qing and H. Qiao-Yun. 2006. Elemental Composition and Geochemical Characteristics of Iron-Manganese Nodules in Main Soils of China. Pedosphere. 16(1): 72 – 81.

White, G. N. and J. B. Dixon. 1996. Iron and manganese distribution in nodules from a young Texas Vertisol. Soil Sci. Soc. Am. J. 60: 1254-1262.

Appendix A. Site Report

Figure A1. Aerial view of Coloso Valley Agricultural Reserve

Figure A2. Soil Map of Coloso Valley Agricultural Reserve

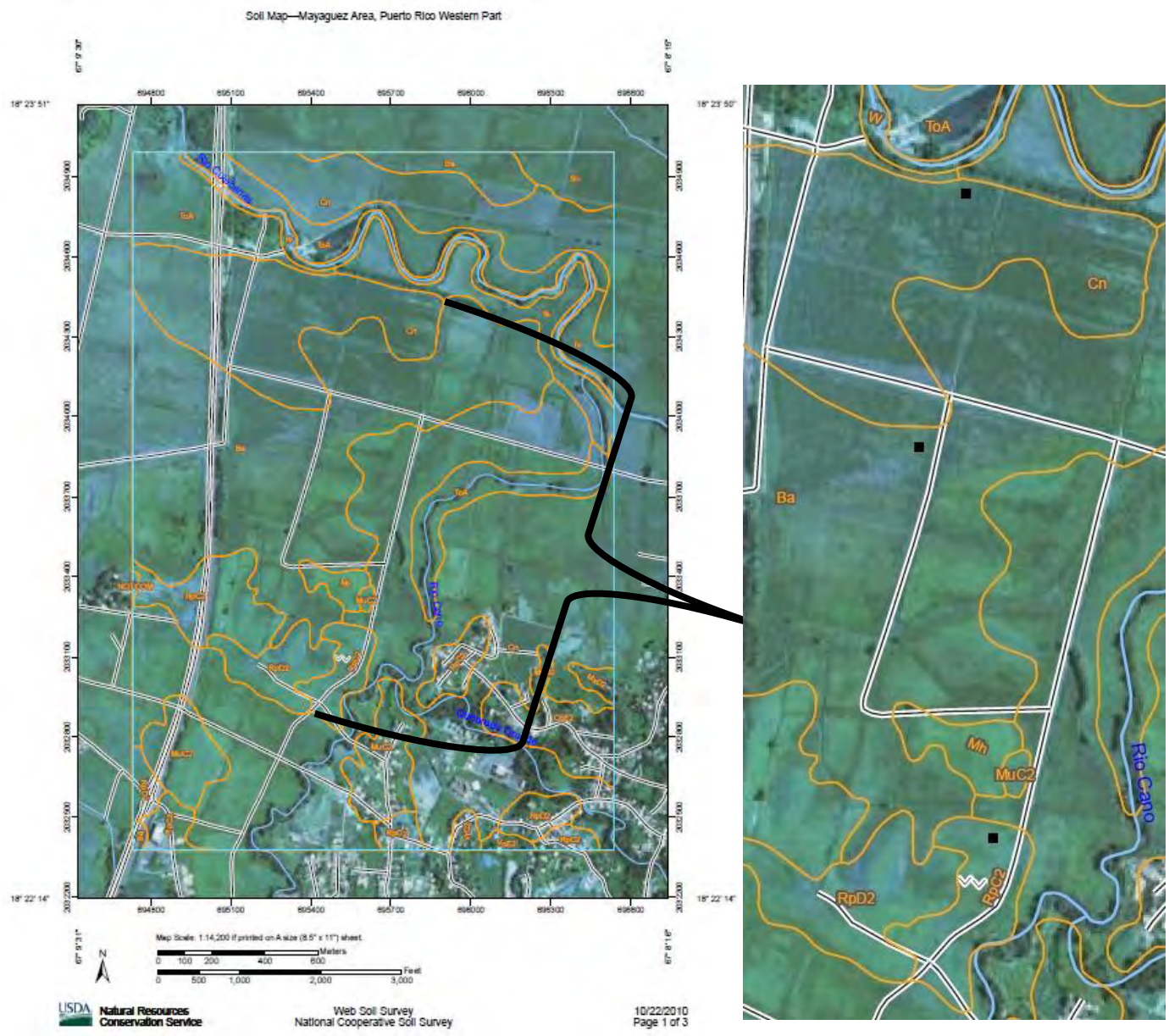

Figure A3. Manganese Nodules in Rio Piedras soil (Crop *Dioscorea esculenta*)

Appendix B. USDA-NRCS Pedon Descriptions

Figure B1. Rio Piedras Pedon Description Part A

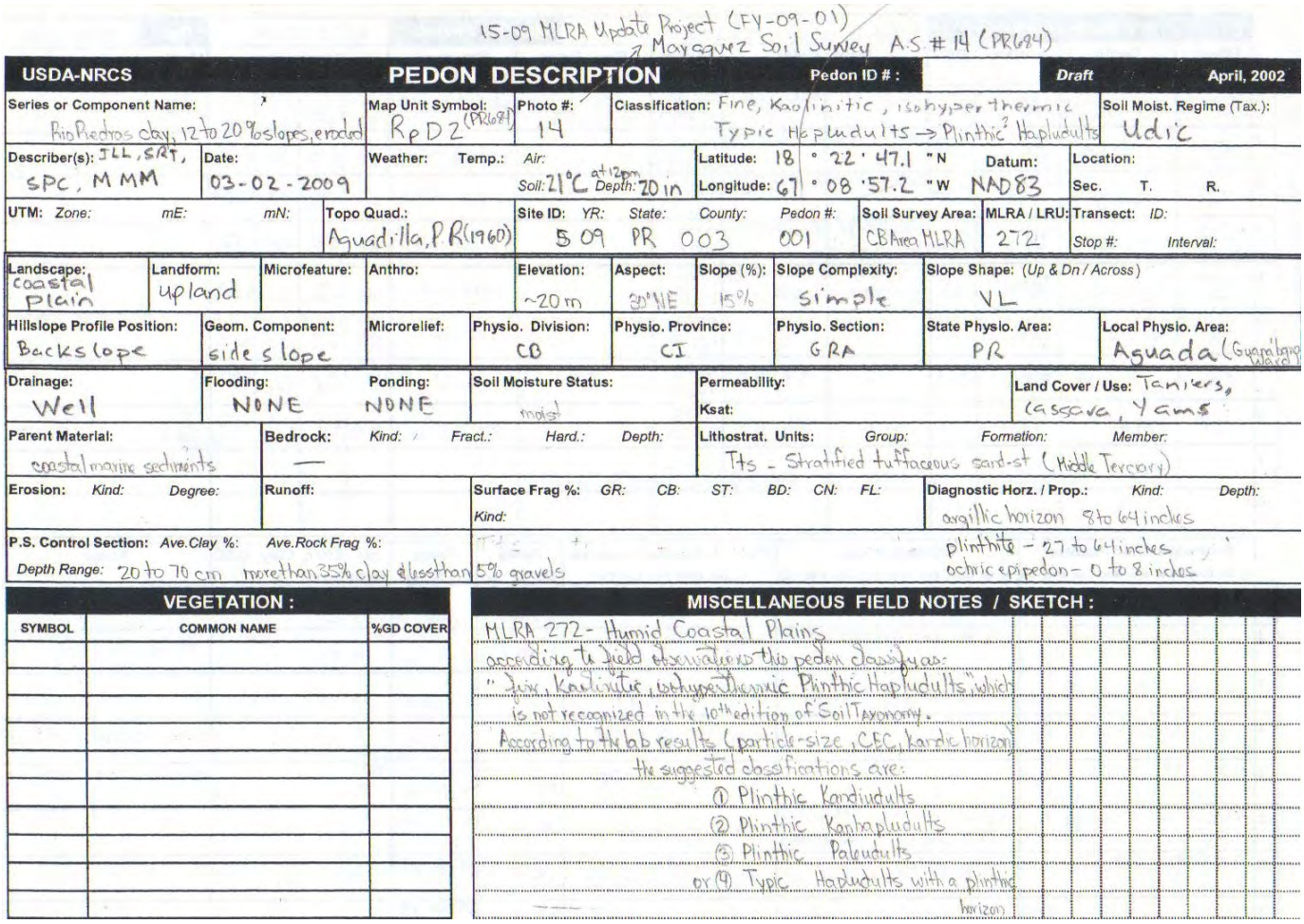

15-09 MLRA Update Project (FY-09-01)
Mayaguez Soil Survey A.S # 14 (PR684)

USDA-NRCS — **PEDON DESCRIPTION** — Pedon ID #: — Draft — April, 2002

Series or Component Name: Rio Piedras clay, 12 to 20 % slopes, eroded	Map Unit Symbol: RpD2 (PR684)	Photo #: 14	Classification: Fine, Kaolinitic, Isohyperthermic Typic Hapludults → Plinthic? Hapludults			Soil Moist. Regime (Tax.): Udic
Describer(s): JLL, SRT, SPC, MMM	Date: 03-02-2009	Weather: Temp.: Air: Soil: 21°C at 12pm Depth: 20 in	Latitude: 18 ° 22 ' 47.1 " N Datum:	Longitude: 67 ° 08 ' 57.2 " W NAD83		Location: Sec. T. R.
UTM: Zone: mE: mN:	Topo Quad.: Aguadilla, PR (1960)	Site ID: YR: State: County: Pedon #: 509 PR 003 001	Soil Survey Area: CB Area MLRA	MLRA / LRU: 272	Transect: ID: Stop #: Interval:	
Landscape: coastal plain	Landform: upland	Microfeature:	Anthro:	Elevation: ~20 m	Aspect: 30° NE	Slope (%): 15%
Slope Complexity: simple	Slope Shape: (Up & Dn / Across) VL					
Hillslope Profile Position: Backslope	Geom. Component: side slope	Microrelief:	Physio. Division: CB	Physio. Province: CI	Physio. Section: GRA	State Physio. Area: PR
Local Physio. Area: Aguada (Guaynabo Ward)						
Drainage: Well	Flooding: NONE	Ponding: NONE	Soil Moisture Status: moist	Permeability: Ksat:	Land Cover / Use: Tanners, cassava, Yams	
Parent Material: coastal marine sediments	Bedrock: Kind: — Fract.: Hard.: Depth:	Lithostrat. Units: Group: Formation: Member: Tts - Stratified tuffaceous sand-st (Middle Tercinary)				
Erosion: Kind: Degree:	Runoff:	Surface Frag %: GR: CB: ST: BD: CN: FL: Kind:	Diagnostic Horz. / Prop.: Kind: argillic horizon	Depth: 8 to 64 inches		
P.S. Control Section: Ave. Clay %: Ave. Rock Frag %: Depth Range: 20 to 70 cm more than 35% clay & less than 5% gravels			plinthite - 27 to 64 inches ochric epipedon - 0 to 8 inches			

VEGETATION :

SYMBOL	COMMON NAME	%GD COVER

MISCELLANEOUS FIELD NOTES / SKETCH :

MLRA 272 - Humid Coastal Plains
according to field observations this pedon classifies as:
"fine, Kaolinitic, isohyperthermic Plinthic Hapludults which is not recognized in the 10th edition of Soil Taxonomy.
According to the lab results (particle-size, CEC, kandic horizon) the suggested classifications are:
① Plinthic Kandiudults
② Plinthic Kanhapludults
③ Plinthic Paleudults
or ④ Typic Hapludults with a plinthic horizon

Figure B2. Rio Piedras Pedon Descirption Part B

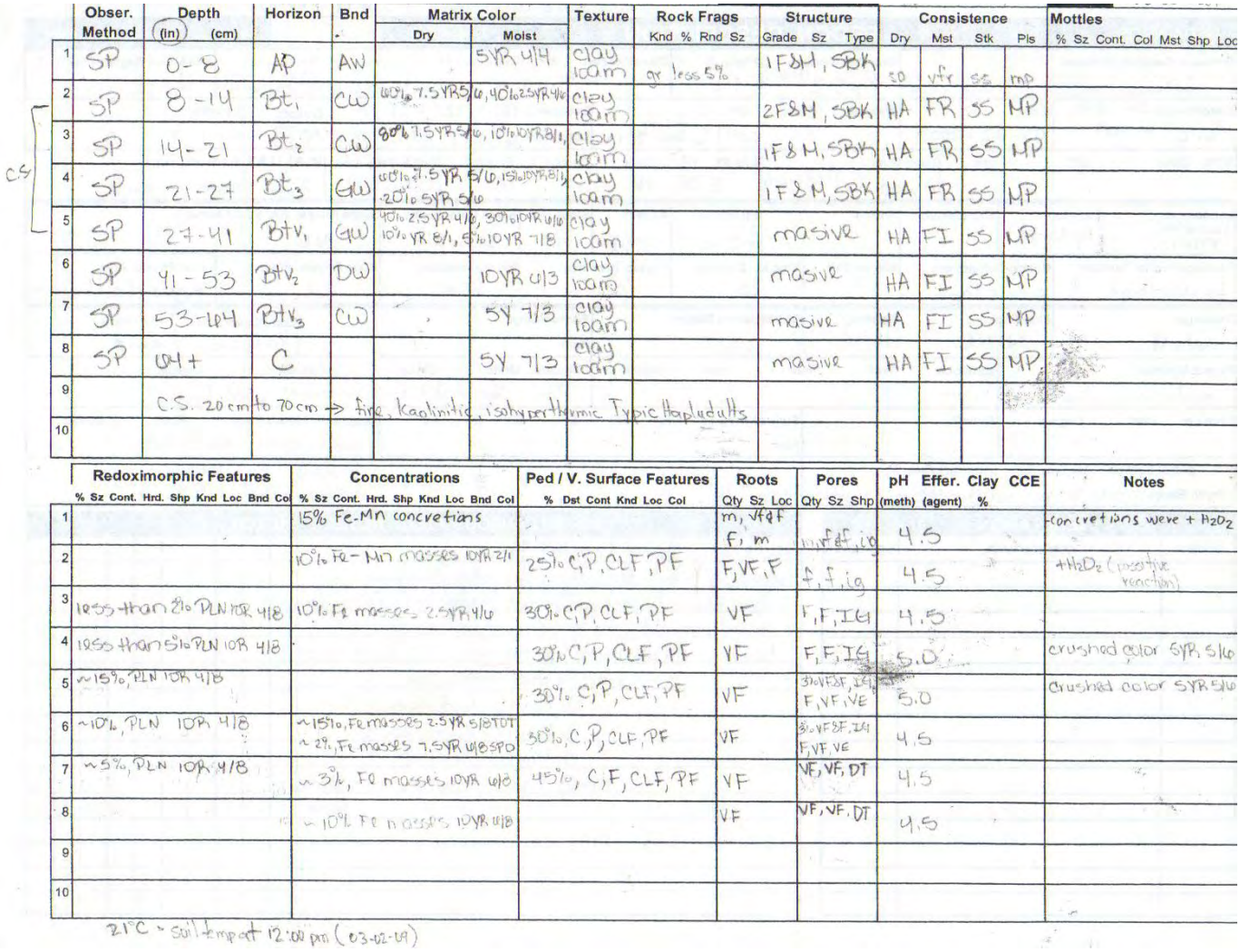

	Obser. Method	Depth (in) (cm)	Horizon	Bnd	Matrix Color Dry	Matrix Color Moist	Texture	Rock Frags Knd % Rnd Sz	Structure Grade Sz Type	Consistence Dry	Consistence Mst	Consistence Stk	Consistence Pls	Mottles % Sz Cont. Col Mst Shp Loc
1	SP	0-8	Ap	AW		5YR 4/4	clay loam	gr less 5%	1FSBK, SBK	SO	vfr	SS	mnP	
2	SP	8-14	Bt_1	CW	60% 7.5YR5/6, 40% 2.5YR4/6		clay loam		2FSBK, SBK	HA	FR	SS	MP	
3	SP	14-21	Bt_2	CW	80% 7.5YR5/6, 10% 10YR8/1,		clay loam		1FSBK, SBK	HA	FR	SS	MP	
4	SP	21-27	Bt_3	GW	60% 7.5YR 5/6, 15% 10YR8/1, 20% 5YR 5/6		clay loam		1FSBK, SBK	HA	FR	SS	MP	
5	SP	27-41	BtV_1	GW	40% 2.5YR 4/6, 30% 10YR 6/6 10% YR 8/1, 5% 10YR 7/8		clay loam		masive	HA	FI	SS	MP	
6	SP	41-53	BtV_2	DW		10YR 6/3	clay loam		masive	HA	FI	SS	MP	
7	SP	53-104	BtV_3	CW		5Y 7/3	clay loam		masive	HA	FI	SS	MP	
8	SP	104+	C			5Y 7/3	clay loam		masive	HA	FI	SS	MP	
9		C.S. 20cm to 70cm → fine, kaolinitic, isohyperthermic Typic Hapludults												
10														

CS

	Redoximorphic Features % Sz Cont. Hrd. Shp Knd Loc Bnd Col	Concentrations % Sz Cont. Hrd. Shp Knd Loc Bnd Col	Ped / V. Surface Features % Dst Cont Knd Loc Col	Roots Qty Sz Loc	Pores Qty Sz Shp	pH (meth)	Effer. (agent)	Clay %	CCE	Notes
1		15% Fe-Mn concretions		m, vf&f F, m		4.5				concretions were + H_2O_2
2		10% Fe-Mn masses 10YR 2/1	25% C,P,CLF,PF	F,VF,F		4.5				+ H_2O_2 (positive reaction)
3	10-55 thin 3% PLN 10R 4/8	10% Fe masses 2.5YR 4/6	30% C,P,CLF,PF	VF	F,F,IG	4.5				
4	10-55 thin 5% PLN 10R 4/8		30% C,P,CLF,PF	VF	F,F,IG	5.0				crushed color 5YR 5/6
5	~15%, PLN 10R 4/8		30% C,P,CLF,PF	VF	30% VFSF,IG F,VF,VE	5.0				crushed color 5YR 5/6
6	~10%, PLN 10R 4/8	~15% Fe masses 2.5YR 5/8 DT ~2% Fe masses 7.5YR 6/8 SPD	30% C,P,CLF,PF	VF	30% VFSF,IG F,VF,VE	4.5				
7	~5%, PLN 10R 4/8	~3% Fe masses 10YR 6/8	45% C,F,CLF,PF	VF	VF,VF,DT	4.5				
8		~10% Fe masses 10YR 6/8		VF	VF,VF,DT	4.5				
9										
10										

21°C - soil temp at 12:00 pm (03-02-04)

Figure B3. Bajura Pedon Description Part A

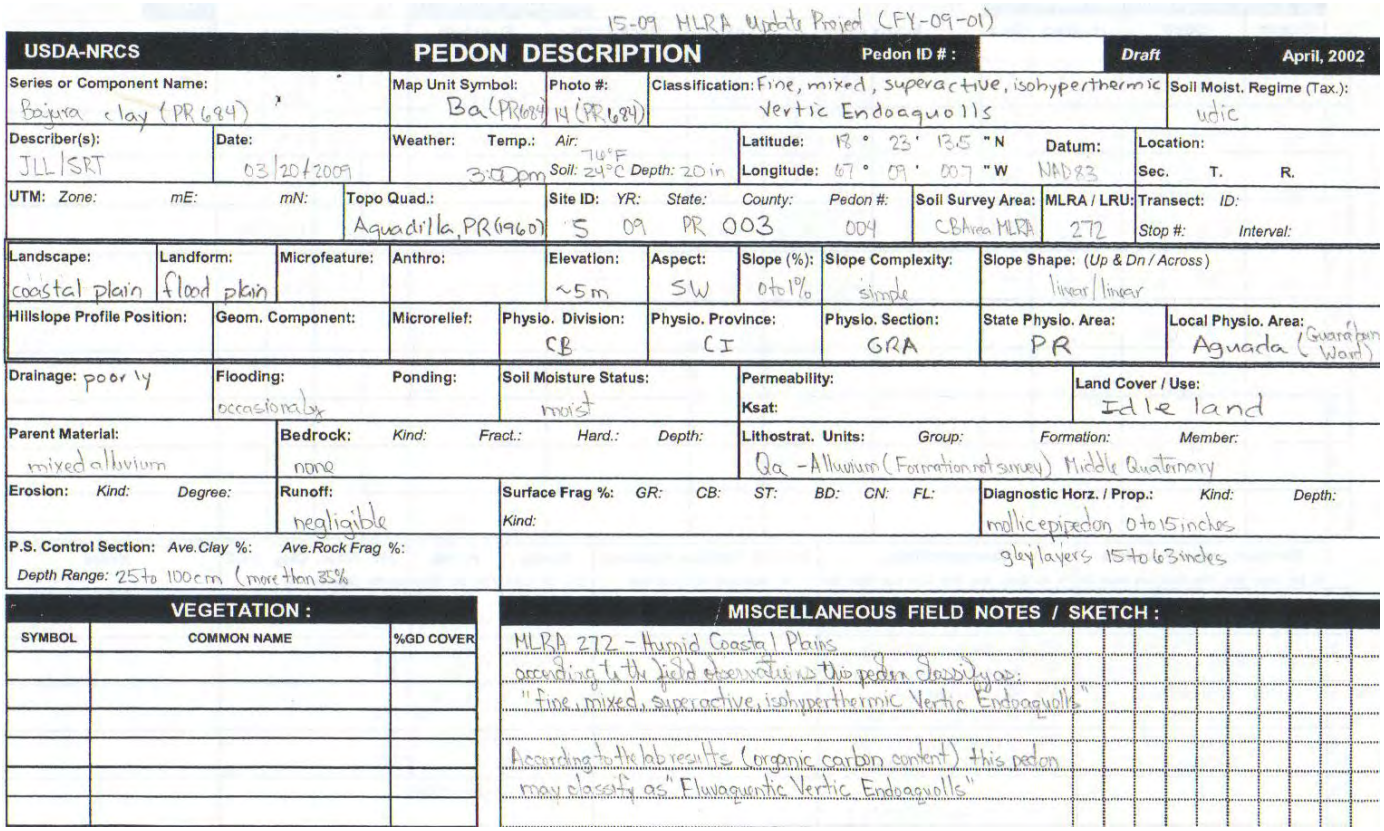

15-09 MLRA Update Project (FY-09-01)

USDA-NRCS — **PEDON DESCRIPTION** — Pedon ID #: — *Draft* — April, 2002

Series or Component Name: Bajura clay (PR684)	Map Unit Symbol: Ba (PR684)	Photo #: 14 (PR684)	Classification: Fine, mixed, superactive, isohyperthermic Vertic Endoaquolls			Soil Moist. Regime (Tax.): udic
Describer(s): JLL/SRT	Date: 03/20/2009	Weather: Temp.: Air: 76°F Soil: 24°C Depth: 20 in 3:00pm	Latitude: 18 ° 23 ' 13.5 " N Datum:	Longitude: 67 ° 09 ' 007 " W NAD83		Location: Sec. T. R.
UTM: Zone: mE: mN:	Topo Quad.: Aguadilla, PR (1960)	Site ID: YR: 5 09 State: PR County: 003 Pedon #: 004	Soil Survey Area: CB Area MLRA	MLRA / LRU: 272		Transect: ID: Stop #: Interval:

Landscape: coastal plain	Landform: flood plain	Microfeature:	Anthro:	Elevation: ~5m	Aspect: SW	Slope (%): 0 to 1%	Slope Complexity: simple	Slope Shape: (Up & Dn / Across) linear/linear
Hillslope Profile Position:	Geom. Component:	Microrelief:	Physio. Division: CB	Physio. Province: CI	Physio. Section: GRA	State Physio. Area: PR	Local Physio. Area: Aguada (Guaraguao Ward)	

Drainage: poorly	Flooding: occasionally	Ponding:	Soil Moisture Status: moist	Permeability: Ksat:
Land Cover / Use: Idle land				

Parent Material: mixed alluvium	Bedrock: Kind: none	Fract.:	Hard.:	Depth:
Lithostrat. Units: Qa - Alluvium (Formation not survey)	Group:	Formation:	Member: Middle Quaternary	

Erosion: Kind: Degree:	Runoff: negligible	Surface Frag %: GR: CB: ST: BD: CN: FL: Kind:	Diagnostic Horz. / Prop.: mollic epipedon 0 to 15 inches	Kind: Depth:
P.S. Control Section: Ave. Clay %: Depth Range: 25 to 100 cm (more than 35%	Ave. Rock Frag %:		gley layers 15 to 63 inches	

VEGETATION :

SYMBOL	COMMON NAME	%GD COVER

MISCELLANEOUS FIELD NOTES / SKETCH :

MLRA 272 - Humid Coastal Plains
according to the field observations this pedon classifys as:
"fine, mixed, superactive, isohyperthermic Vertic Endoaquolls"

According to the lab results (organic carbon content) this pedon may classify as "Fluvaquentic Vertic Endoaquolls"

Figure B4. Bajura Pedon Description Part B

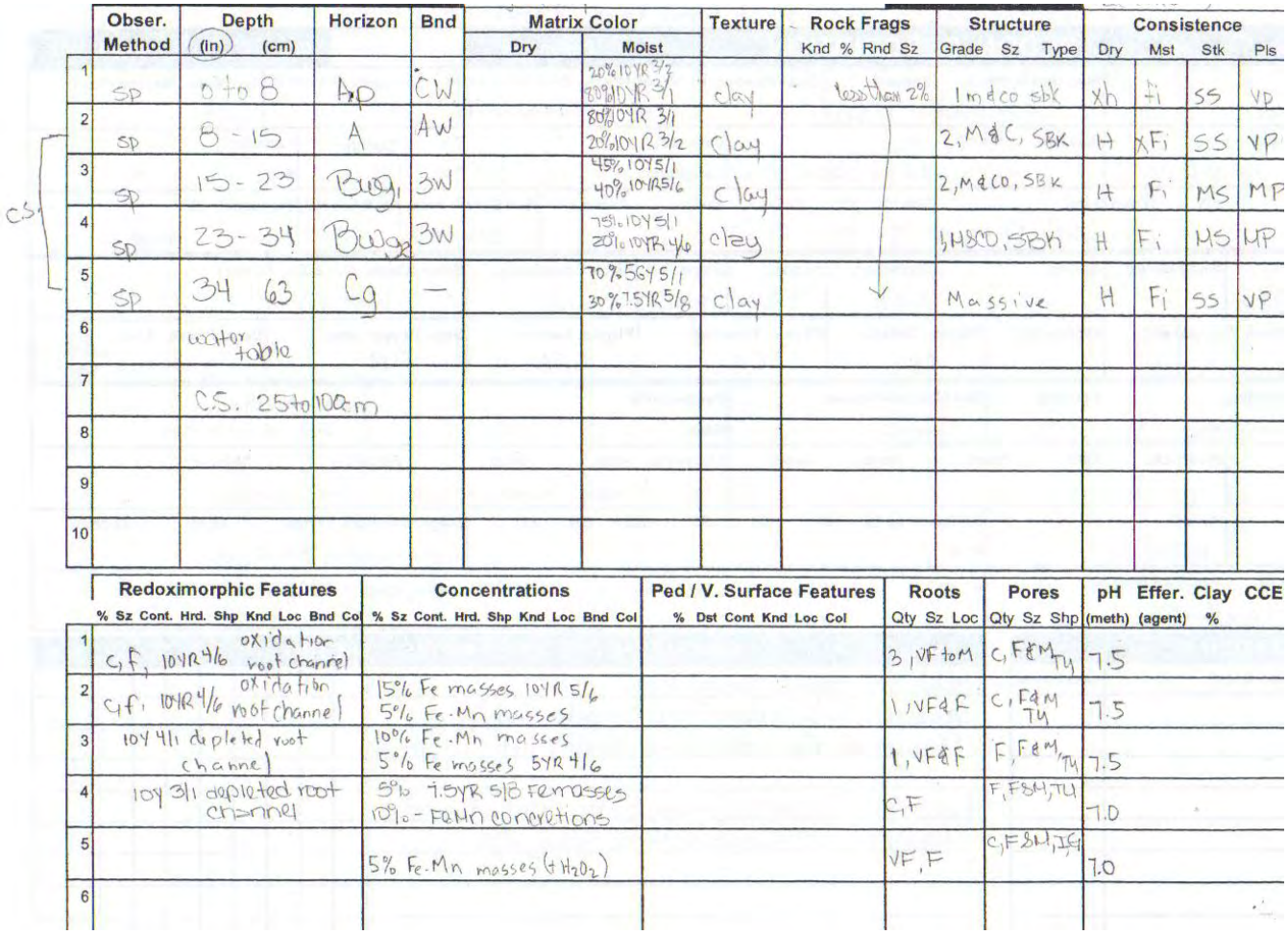

	Obser. Method	Depth (in) (cm)	Horizon	Bnd	Matrix Color Dry	Matrix Color Moist	Texture	Rock Frags Knd % Rnd Sz	Structure Grade Sz Type	Consistence Dry	Mst	Stk	Pls
1	sp	0 to 8	Ap	CW		20% 10YR 3/3 80% 10YR 3/1	clay	less than 2%	1 m d co sbk	xh	fi	ss	vp
2	sp	8 - 15	A	AW		80% 10YR 3/1 20% 10YR 3/2	clay		2, M & C, SBK	H	xFi	SS	VP
3	sp	15 - 23	Bwg1	3W		45% 10Y 5/1 40% 10YR 5/6	clay		2, M & CO, SBK	H	Fi	MS	MP
4	sp	23 - 34	Bwg2	3W		75% 10Y 5/1 20% 10YR 4/6	clay		1, M & CO, SBK	H	Fi	MS	MP
5	sp	34 63	Cg	—		70% 5GY 5/1 30% 7.5YR 5/8	clay		Massive	H	Fi	ss	VP
6		water table											
7		C.S. 25 to 100 cm											
8													
9													
10													

CS

	Redoximorphic Features % Sz Cont. Hrd. Shp Knd Loc Bnd Col	Concentrations % Sz Cont. Hrd. Shp Knd Loc Bnd Col	Ped / V. Surface Features % Dst Cont Knd Loc Col	Roots Qty Sz Loc	Pores Qty Sz Shp	pH (meth)	Effer. (agent)	Clay %	CCE
1	C, f, 10YR 4/6 oxidation root channel			3, VF to M	C, F&M TU	7.5			
2	C, f, 10YR 4/6 oxidation root channel	15% Fe masses 10YR 5/6 5% Fe-Mn masses		1, VF&F	C, F&M TU	7.5			
3	10Y 4/1 depleted root channel	10% Fe-Mn masses 5% Fe masses 5YR 4/6		1, VF&F	F, F&M, TU	7.5			
4	10Y 3/1 depleted root channel	5% 7.5YR 5/8 Fe masses 10% - Fe-Mn concretions		C, F	F, F&M, TU	7.0			
5		5% Fe-Mn masses (+ H_2O_2)		VF, F	C, F&M, TU	7.0			
6									

Figure B5. Coloso Pedon Description Part A

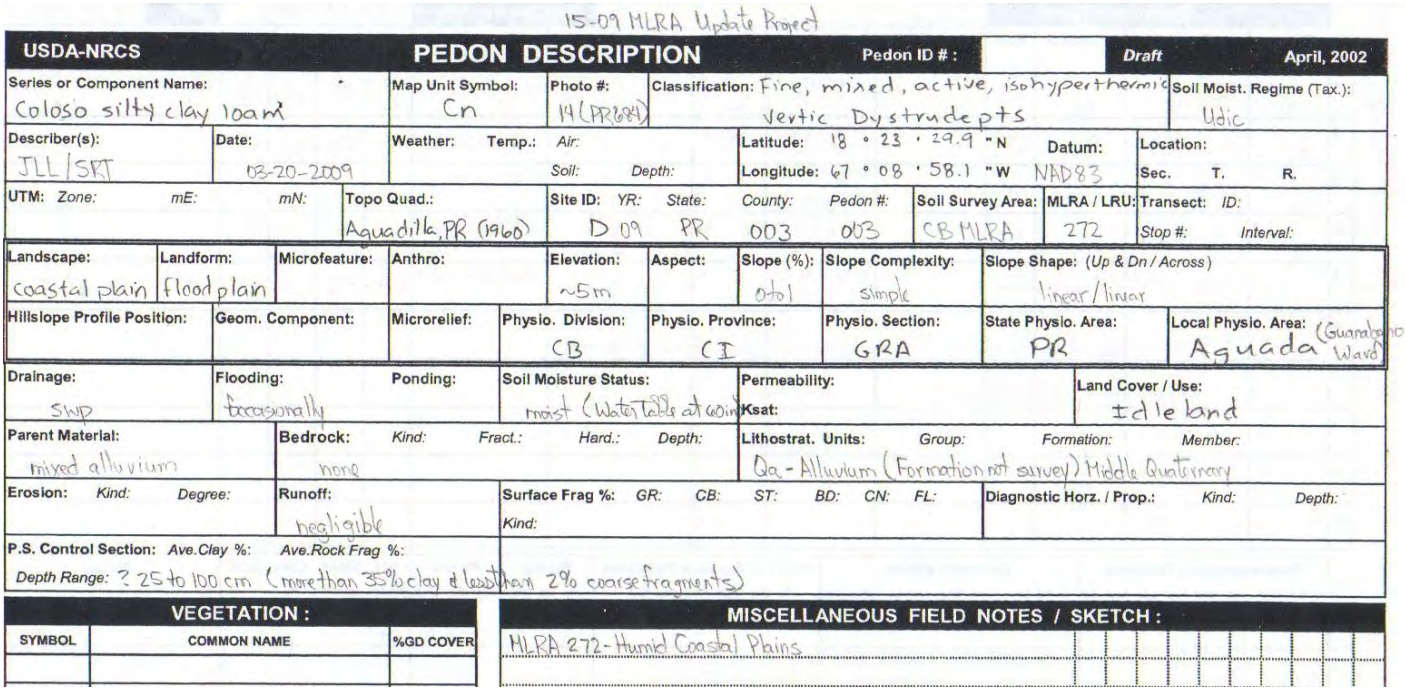

15-09 MLRA Update Project

USDA-NRCS — **PEDON DESCRIPTION** — Pedon ID # : — *Draft* — April, 2002

Series or Component Name: Coloso silty clay loam		Map Unit Symbol: Cn	Photo #: 14 (PR688)	Classification: Fine, mixed, active, isohyperthermic Vertic Dystrudepts					Soil Moist. Regime (Tax.): Udic
Describer(s): JLL/SRT	Date: 03-20-2009	Weather: Temp.: Air: Soil: Depth:		Latitude: 18 ° 23 ' 29.9 " N Longitude: 67 ° 08 ' 58.1 " W		Datum: NAD83	Location: Sec. T. R.		
UTM: Zone: mE: mN:		Topo Quad.: Aguadilla, PR (1960)	Site ID: YR: State: D 09 PR	County: 003	Pedon #: 003	Soil Survey Area: CB MLRA	MLRA / LRU: 272	Transect: ID: Stop #: Interval:	
Landscape: coastal plain	Landform: floodplain	Microfeature:	Anthro:	Elevation: ~5m	Aspect:	Slope (%): 0 to 1	Slope Complexity: simple	Slope Shape: (Up & Dn / Across) linear / linear	
Hillslope Profile Position:	Geom. Component:	Microrelief:	Physio. Division: CB	Physio. Province: CI	Physio. Section: GRA	State Physio. Area: PR	Local Physio. Area: Aguada (Guanajibo Ward)		
Drainage: SWP	Flooding: occasionally	Ponding:	Soil Moisture Status: moist (Water table at 60in)	Permeability: Ksat:		Land Cover / Use: Idle land			
Parent Material: mixed alluvium	Bedrock: Kind: none	Fract.:	Hard.:	Depth:	Lithostrat. Units: Qa - Alluvium (Formation not survey)	Group:	Formation:	Member: Middle Quaternary	
Erosion: Kind: Degree:	Runoff: negligible	Surface Frag %: GR: CB: ST: BD: CN: FL: Kind:			Diagnostic Horz. / Prop.:	Kind:	Depth:		
P.S. Control Section: Ave. Clay %: Ave. Rock Frag %: Depth Range: ? 25 to 100 cm (more than 35% clay & less than 2% coarse fragments)									

VEGETATION :

SYMBOL	COMMON NAME	%GD COVER

MISCELLANEOUS FIELD NOTES / SKETCH :

MLRA 272 - Humid Coastal Plains

Figure B6. Coloso Pedon Description Part B

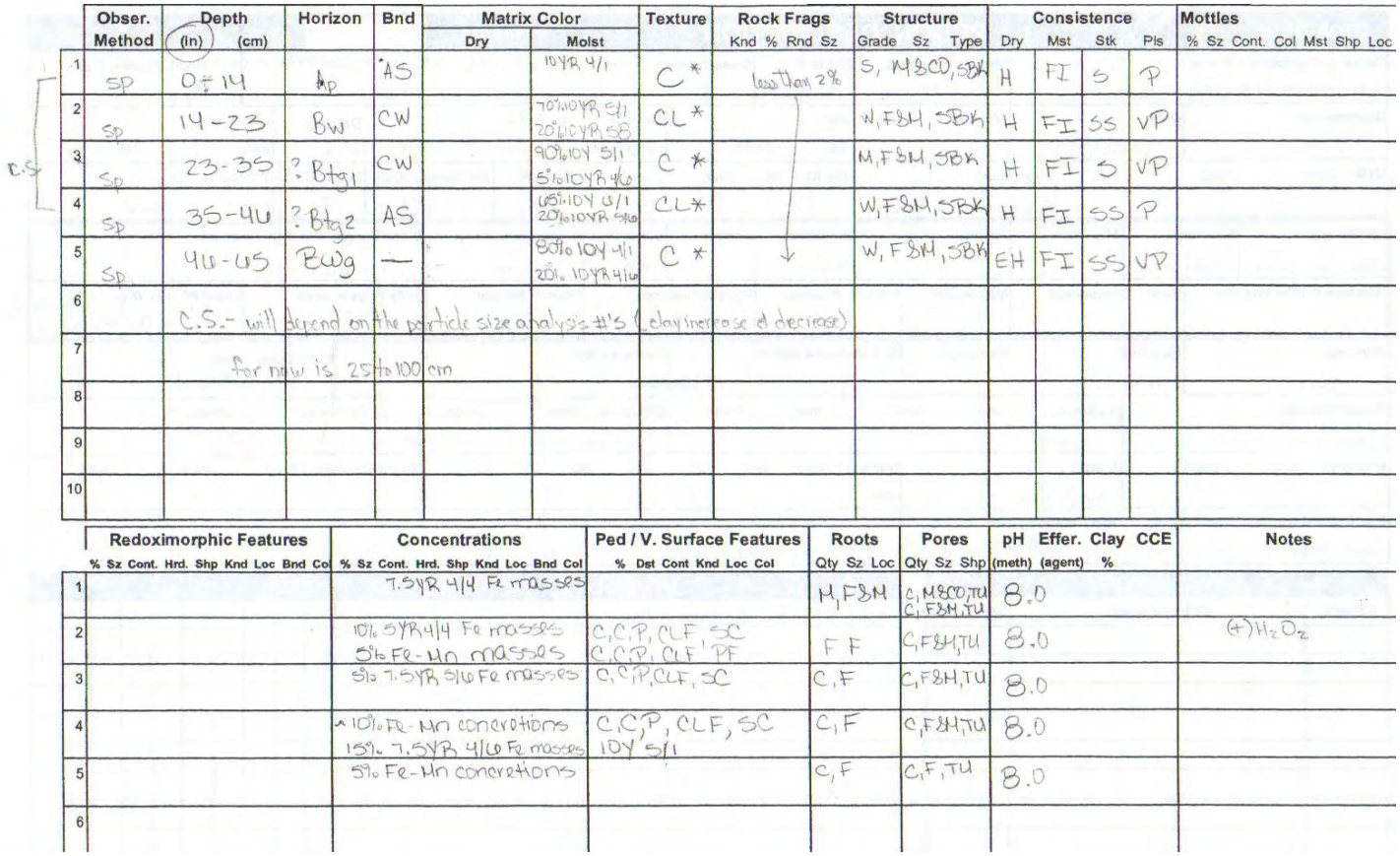

	Obser. Method	Depth (in)	Depth (cm)	Horizon	Bnd	Matrix Color Dry	Matrix Color Moist	Texture	Rock Frags Knd % Rnd Sz	Structure Grade Sz Type	Consistence Dry	Consistence Mst	Consistence Stk	Consistence Pls	Mottles % Sz Cont. Col Mst Shp Loc
1	SP	0 ± 14		Ap	AS		10YR 4/1	C *	less than 2%	S, M SBK, SBK	H	FI	S	P	
2	SP	14-23		Bw	CW		70% 10YR 5/1 20% 10YR 5/8	CL *		W, F SBK, SBK	H	FI	SS	VP	
3	SP	23-35		? Btg1	CW		90% 10Y 5/1 5% 10YR 4/6	C *		M, F SBK, SBK	H	FI	S	VP	
4	SP	35-46		? Btg2	AS		65% 10Y 5/1 20% 10YR 5/6	CL *		W, F SBK, SBK	H	FI	SS	P	
5	SP	46-65		BWg	—		80% 10Y 4/1 20% 10YR 4/6	C *		W, F SBK, SBK	EH	FI	SS	VP	
6		C.S.- will depend on the particle size analysis #'s (clay increase & decrease)													
7		for now is 25 to 100 cm													
8															
9															
10															

C.S.

	Redoximorphic Features % Sz Cont. Hrd. Shp Knd Loc Bnd Col	Concentrations % Sz Cont. Hrd. Shp Knd Loc Bnd Col	Ped / V. Surface Features % Dst Cont Knd Loc Col	Roots Qty Sz Loc	Pores Qty Sz Shp	pH (meth)	Effer. (agent)	Clay %	CCE	Notes
1		7.5YR 4/4 Fe masses		M, F SH	C, M SCO, TU C, F SH, TU	8.0				
2		10% 5YR 4/4 Fe masses 5% Fe-Mn masses	C, C, P, CLF, SC C, C, P, CLF, PF	F F	C, F SH, TU	8.0				(+) H_2O_2
3		5% 7.5YR 5/6 Fe masses	C, C, P, CLF, SC	C, F	C, F SH, TU	8.0				
4		~10% Fe-Mn concretions 15% 7.5YR 4/6 Fe masses	C, C, P, CLF, SC 10Y 5/1	C, F	C, F SH, TU	8.0				
5		5% Fe-Mn concretions		C, F	C, F, TU	8.0				
6										

Appendix C. USDA-NRCS Soil Characterization Report

USDA-NRCS MLRA 15-9 Soil Survey Office

Rio Piedras Series

Control Section: 25 to 100 cm (10 to 40 inches)
According to the S09PR-003001 (Thermal Analysis) the mineralogy is kaolinitic.
14 to 21 inches (Bw_2) 57% kaolinitic and 4% gibbsite
21 to 27 inches (Bw_3) 56% kaolinitic and 3% gibbsite
http://ssldata.nrcs.usda.gov/rptExecute.asp?p=40146&r=1&r=2&r=3&submit1=Get+Report
The soil temperature regime in this area is isohyperthermic (above 22° C) and the difference between the Mean Summer and the Mean Winter Soil is 6°C or less (Lugo-Camacho, J.L., 2005. The Soil Climate Regimes of Puerto Rico-Reassessment and Implications. M.S. Thesis. Department of Agronomy and Soil Science; University of Puerto Rico-Mayagüez). http://grad.uprm.edu/tesis/lugocamacho.pdf
The Soil Moisture Regime is Udic (http://grad.uprm.edu/tesis/lugocamacho.pdf)

Bajura Series

Control Section: 25 to 100 cm (10 to 40 inches)

According to the S09PR-003004 (Thermal Analysis) the mineralogy is kaolinitic.

14 to 23 inches (Bwg_1) 63% kaolinitic and 5% gibbsite

http://ssldata.nrcs.usda.gov/rptExecute.asp?p=40147&r=1&r=2&r=3&submit1=Get+Report

The soil temperature regime in this area is isohyperthermic (above 22° C) and the difference between the Mean Summer and the Mean Winter Soil is 6°C or less (Lugo-Camacho, J.L., 2005. The Soil Climate Regimes of Puerto Rico-Reassessment and Implications. M.S. Thesis. Department of Agronomy and Soil Science; University of Puerto Rico-Mayagüez). http://grad.uprm.edu/tesis/lugocamacho.pdf

The Soil Moisture Regime is Udic (http://grad.uprm.edu/tesis/lugocamacho.pdf)

Redoximorphic features from 0 to 63 inches and over .2 percent or more organic carbon content (or an irregular decrease) (Holocene age) at 125 cm below the mineral soil surface and less than 25% slopes in the landscape.

S09PR-00304 Bajura Series						
Soil Organic Carbon						
Former Horizon Designation	Current Horizon Designation	Total Carbon (%)	Soil Organic Carbon (%)	Conversion Factor	Organic Matter (%)	
Ap	Ap	2.36	2.36	1.72	4.069	
A	AB	1.22	1.22	1.72	2.103	
Bwg_1	Bwg_1	0.59	0.59	1.72	1.017	
Bwg_2	Bwg_2	0.39	0.39	1.72	0.672	
Cg	Cg	0.31	0.31	1.72	0.534	

Although this pedon have 100% base saturation and the colors required for the Mollic epipedon the A and AB horizons consistence is extremely hard and respectively, therefore this pedon meet the criteria for an ochric epipedon.

Coloso Series

Control Section: 25 to 100 cm (10 to 40 inches)

According to the S05PR-003001R the mineralogy is kaolinitic (as recommended by the National Soil Survey Lab according to the S09PR003004 Thermal Analysis Data (http://ssldata.nrcs.usda.gov/rptExecute.asp?p=40147&r=1&r=2&r=3&submit1=Get+Report).

http://ssldata.nrcs.usda.gov/rptExecute.asp?p=32621&r=1&submit1=Get+Report (Coloso)

The soil temperature regime in this area is isohyperthermic (above 22° C) and the difference between the Mean Summer and the Mean Winter Soil is 6°C or less (Lugo-Camacho, J.L., 2005. The Soil Climate Regimes of Puerto Rico-Reassessment and Implications. M.S. Thesis. Department of Agronomy and Soil Science; University of Puerto Rico-Mayagüez).

Linear Extensibility = depth x COLE

D09PR-003003 Coloso Series						
Linear Extensibility (S05PR-003001R data)						
Horizon	**Depth (cm)**	**Cole**	**Depth * Cole**			
Bw_1	3	0.129	0.387			
Bw_2	18	0.119	2.142			
Bw_3	15	0.137	2.055			
C	36	0.111	3.996			
2Cssg	3	0.137	0.411			
	75		8.991	9.0		Vertic

According to the S05PR-003001R results the Linear extensibility in the Control Section is 9.0 therefore the soil is Vertic.

Jorge Leonardo Lugo-Camacho
MLRA Soil Scientist Project Leader